Index

This .pdf file contains

- the point-by-point responses to the reviews
- a marked-up manuscript version showing the changes made

separated by blank pages.

Extensive changes have been necessary considering the Referee's suggestion to repeat the model simulations with more reference stations and an updated meteorology. That is why the versions are hard to compare and the Figures to some extend had to be replaced and renumbered.
We apologize for the inconvenience.

We thank the referee for the comments.
Here the comments are listed (black) with our reply (red, italics).

General comments

The discussion paper of Zimmermann et al. presents an analysis of the global budget and trends of atmospheric CH4 for the period 1997-2014, using the EMAC atmospheric chemistry general circulation model. As such the study contributes to the highly controversial discussion on the drivers of the renewed increase of atmospheric CH4 observed since 2007, and is well within the scope of ACP. However, there are several significant limitations of the study, which limit the conclusions that can be drawn from the presented results.

Following the referee's advice, most points of criticism have been taken into account and new simulation runs have been performed:

(1) The study uses only a very limited number of atmospheric stations.

Indeed only a limited amount of stations were used in the comparison. Following the referee's advice, the simulation was repeated using 16 NOAA stations and CGO (AGAGE):

Code	Station Name	Country	Lat °	Lon °	elevation / m
ALT	Alert	Canada	82.45	-62.51	190
ASC	Ascension Island	UK	-7.97	-14.40	85
AZR	Terceira Ile., Azores	Portugal	38.77	-27.38	19
BRW	Barrow, Alaska	USA	71.32	-156.61	11
CGO	Cape Grim, Tasmania	Australia	-40.68	144.69	94
CRZ	Crozet Island	France	-46.43	51.85	197
EIC	Easter Island	Chile	-27.16	-109.43	47
GMI	Mariana Islands	Guam	13.39	144.66	0
HBA	Halley Station,	Antarctica, UK	-75.61	-26.21	30
MLO	Mauna Loa, Hawaii	USA	19.54	-155.58	3397
RPB	Ragged Point	Barbados	13.17	-59.43	15
SEY	Mahe Island,	Seychelles	-4.68	55.53	2
SHM	Shemya Island, Alaska	USA	52.71	174.13	23
SMO	Tutuila, Am. Samoa	USA	-14.25	-170.56	42
SPO	South Pole	USA	-89.98	-24.80	2810
ZEP	Ny-Alesund, Svalbard	Norway, Sweden	78.91	11.89	474

In fact, only one single NOAA station (MLO) has been used (in addition to the 5 AGAGE stations). These 5+1 stations cover only the latitude range between 53oN and 41oS. It is not clear, why the authors do not use any data from the comprehensive NOAA ESRL global cooperative air sampling network (nor from the second NOAA station with continuous CH4 measurements at Barrow, Alaska). The very limited set of stations used in this study limits the information that can be obtained on the CH4 emissions at continental scale.

(2) 4 of the 6 stations used in this study are coastal sites (MHD, THD, RPB, CGO).
Using such data requires that the model can properly simulate synoptic scale variability
(e.g. change between marine and continental air masses).

We thank the referee for pointing this out.
In the new simulation all stations are "clean air" sites and filtered wrt synoptic scale pollution (except CGO).
We also revised the text in Ch. 3.1:
"The data provided (Dlugokencky et al., 2018) are filtered with respect to synoptic scale pollution events. We take advantage of 16 stations about fairly equally distributed over the globe (Fig. 2a) and remote from the major emission areas to ensure comparability with the model results which are not filtered. For the same reason, in case of Cape Grim, Australia (41° S, 145°) we refer to the unfiltered AGAGE records (Prinn et al., 1978, 2013). At all stations monthly mean mixing-ratios are compared to respective monthly averaged model samples. "

Our actual model resolution "T106" with a grid size of 125 km at the Equator is able to capture also synoptic scale events; however the fifteen NOAA stations that we used are remote from the main source regions. CGO is influenced my air from the Australian continent but the model is able to reproduce eventual pollution events.

The EMAC model, however, is a general circulation model, and - as described in the paper – nudged to ECMWF meteorology only in the free troposphere (apart from surface pressure).
Therefore, the capability of the EMAC model to simulate synoptic variability is probably worse compared to offline atmospheric transport models which are directly driven by analyzed meteorological fields.

Indeed, we operate the EMAC GCM/CCM in "nudged" mode, i.e. by Newtonian relaxation towards ECMWF meteorology. The nudging (of divergence, vorticity, temperature (excluding global mean) and logarithm of surface pressure) is applied in spectral space, however (by so-called low normal mode insertion) only down to the synoptic scale. Thus, the meteorological sequence of ECMWF is reproduced by EMAC on the synoptic scale, whereas the variability on sub-synoptic scale is determined by the model physics (e.g. convection etc.).
Thus, the synoptic variability should not be an issue here.

Good model representation of the continental stations, however, is essential for the study, since the is derived as "as the difference between average CH4 mixing-ratios at the northern stations MHD (53oN) and THD (41oN) and the southern station CGO (41oS)" (lines 302-304) - and the interhemispheric gradient derived in this way is used to optimize the contribution from the "tropical wetland source (SWA)" and "landfill-, coal-, gas-, and oil (FOS)" emissions.

Following the referee's advice, in the new simulation we are using an improved interhemispheric gradient definition and define:
ΔNH/SH = avg(ALT, ZEP, BRW) minus avg(CGO, CRZ, HBA, SPO).

Furthermore the contributions of all (10) emission categories are now explicitly considered in the optimization procedure.

Related to the concern of the potential limitations of the EMAC model to simulate the synoptic variability is the fact that the study uses "Monthly mean mixing - unfiltered with respect to local pollution events" (lines 205-206) measurements, which are compared to monthly mean model output. Especially for the 4 coastal sites, it would be more appropriate to use hourly (or daily) observations. If the EMAC model cannot properly simulate these sites, the use of monthly mean values for the comparison is likely to result in biased results.
As mentioned above, the sites have changed in the new simulation.
Consistently with the measurements, the model now samples at every time step and averages at the end of every month (sub-model SCOUT).

(3) Unfortunately, the study investigates only 2 scenarios to analyze the recent CH4 trend: (1) scenario "TRO" with additional emissions from the tropical wetlands, and (2) scenario "SHA" with additional emissions from the North American shale gas drilling sites. However, further hypotheses have been proposed in the literature, including increasing CH4 emissions from agriculture and waste sectors [Saunois et al., 2017; Schaefer et al., 2016], and decreasing CH4 emissions from biomass burning [Saunois et al., 2017; Worden et al., 2017].

We do not discriminate the latter sectors in this study. It has been our intension to test the sensitivity of the station- and flight records to the hypothetical TRO and SHA emission assumptions.
Biomass burning emissions are not considered in the trend phase.
We take advantage of GFED4.1s which includes agricultural waste burning. No persistent decrease is obvious in this dataset (Fig. 1 at the end of this document.)

While the decreasing _13CH4 observed in the atmosphere points to an increasing microbial sources (including both wetlands and anthropogenic microbial sources), Saunois et al. [2017] and Schaefer et al. [2016] concluded that among the microbial sources agriculture and waste sectors are more important than natural wetlands.
It is not possible to resolve the latter sectors in the current model setup. The referee's advice will be subject to further investigation also considering observations beyond 2016.

This hypothesis is also supported by statistical data which suggest a significant increase of global CH4 emission from enteric fermentation and manure by 10 Tg CH4 yr-1 between 2000 and 2011 ([Saunois et al., 2017], Fig. S12). The magnitude of the estimated decrease in biomass burning is smaller (estimated to be 3.7 (±1.4) Tg CH4 per year from the 2001–2007 to the 2008–2014 period [Worden et al., 2017]), but plays an essential role for the _13CH4 budget and to reconcile the different hypotheses about the recent CH4 increase.
Based on these general comments, I recommend to thoroughly revise the study, analyzing in more detail the capability of EMAC to simulate synoptic scale variability, to use a more comprehensive set of surface observations,

Following the referee's advice we revised the study and performed new simulations.
and to include additional scenarios (in particular including the increase of CH4 emissions from agricultural sources).

It has been our aim from the beginning to test how well the taken assumptions (in form of given emission datasets of 10 categories) can explain the observations. Realizing a significant underestimation from 2007 on, the two hypothetical scenarios TRO and SHA have been included for sensitivity testing of the observed trend.

Further specific comments:
Abstract, line 21: I would suggest to replace "atmospheric CH4 calculations" by "atmospheric CH4 concentrations" or "atmospheric CH4 dry air mole fractions"
Ok: "The atmospheric CH_4 dry air mole fractions . . ."

Abstract, line 24: "rescaling of individual emissions with proportional effects on the corresponding inventories": it is not clear what is meant here with "inventories" as compared to the "emissions".
New formulation: "... rescaling of individual emissions with proportional effects on respective source segregated methane abundances."

Abstract, line 27: "all-station mean dry air mole fraction of 1792 nmol/mol": reference time period should be given (is this the 2000-2005 period mentioned in the following sentence, or the 1997-2006 period mentioned earlier?).
New formulation: ". . . the 2000 – 2005 observed all-station mean dry air mole fraction of 1780 nmol/mol could be reproduced within an RMS = 0.40 % . . ."

Abstract, line 38: "The coefficient of determination of R2 = 0.91 indicates even higher significance than before 2006": This could be partly due a larger range of concentrations values (and the given RMS is slightly higher than before 2006, indicating rather slightly poorer agreement).
In the new simulation including 16 ground stations we had to update the statistics:
"We explored the contributions of two potential causes, one representing natural emissions from wetlands in the tropics "TRO", and the other anthropogenic (e.g. shale gas fracturing) emissions in North America "SHA". Based on the acceptance of the no-trend period emission distribution, with the Solver we estimated annual 19.4 TRO and 5.7 Tg/y SHA contributions, respectively, to optimally fit the trend (RMS = 0.55 % / R^2 = 0.88). "

Abstract, line 40-41: "...indicating that the model reproduces the seasonal and synoptic variability of CH4 in the upper troposphere and lower stratosphere." The analysis in the paper shows also clear limitations to simulate the variability in the lower stratosphere. This should be mentioned also in the abstract.
Following the referee's advice we included the following statement:
"The coefficient of determination R^2 implies that the model reproduces the seasonal and synoptic variability of CH_4 in the UTLS. Regression analysis however indicates evident underestimation of the calculated CH_4 variability, suggesting that the vertical resolution of the model grid is not optimal to resolve the fine structure in the tropopause region. "

Introduction, lines 45-46: "and its concentration has been growing by about 1%/y since the beginning of the Anthropocene in the 19th century (Crutzen, 2002)": I would suggest to add further references for the atmospheric CH4 increase.
Following the referee's advice we included: "Clais et al. 2013"

Reference: Ciais, P., C. Sabine, G. Bala, L. Bopp, V. Brovkin, J. Canadell, A. Chhabra, R. DeFries, J. Galloway, M. Heimann, C. Jones, C. Le Quéré, R.B. Myneni, S. Piao and P. Thornton, 2013: Carbon and Other Biogeochemical Cycles. In: Climate Change 2013: The Physical Science Basis. Contribution of Working Group I to the Fifth Assessment Report of the Intergovernmental Panel on Climate Change [Stocker, T.F., D. Qin, G.-K. Plattner, M. Tignor, S.K. Allen, J. Boschung, A. Nauels, Y. Xia, V. Bex and P.M. Midgley (eds.)]. Cambridge University Press, Cambridge, United Kingdom and New York, NY, USA.

Introduction, lines 47-50: I would propose to present here mainly the most recent estimates of the radiative forcing. If the authors want to include also the older estimates, they should briefly explain the reasons for the large differences in the estimates. Furthermore, the given values "0.57 Wm−2 (direct 0.44Wm−2, indirect 0.13Wm−2)" are not consistent with the given [Dlugokencky et al., 2011] reference (where higher values are reported).

Following the referee's advice we included:

"The resulting factor of 2.5 increase in the global abundance of atmospheric methane (CH_4) since 1750 contributes 0.5 Wm^{-2} to total direct radiative forcing by long-lived greenhouse gases (2.77 Wm^{-2} in 2009), while its role in atmospheric chemistry adds another approximately 0.2 Wm^{-2} of indirect forcing (Dlugokencky et al., 2011) Etminan et al, (2016) presented new calculations including the impact of the shortwave forcing and found that the 1750–2011 radiative forcing is about 25% higher (increasing from 0.48Wm−2 to 0.61Wm−2) compared to the value in the Intergovernmental Panel on Climate Change (IPCC) 2013 assessment."

Reference: Etminan, M., G. Myhre, E. J. Highwood, and K. P. Shine (2016), Radiative forcing of carbon dioxide, methane, and nitrous oxide: A significant revision of the methane radiative forcing, Geophys. Res. Lett., 43, 12,614 – 12,623, doi:10.1002/2016GL071930.

Introduction, lines 52-53: "...in 2007 the CH4 increase resumed unexpectedly (Bergamaschi et al., 2013)": Include here the primary references reporting the CH4 increase from the measurements ([Dlugokencky et al., 2009; Rigby et al., 2008]).

Following the referee's advice we included these references:

"The resuming upward trend after 2007 (Dlugokencky et al., 2009; Rigby et al., 2008, IPCC 2014) is not fully understood: data analysis (Nisbet et al., 2016, Worden et al., 2017) and inverse modelling studies (Bergamaschi et al., 2013) indicate…"

Introduction, lines 72-73: "Schaefer et al. (2016)... raising concern about the contribution from rice production versus wetland emissions". It should be mentioned here that Schaefer et al. (2016) conclude that the increase could be largely explained by increase of CH4 emissions from ruminants (see also my general comment (3)): " Inventories report increased annual agricultural emissions over the 2000-2006 average of 12 Tg by 2011; dominated by ruminants (21, 23). This can largely account for the post-2006 [CH4]-growth, estimated at 15-22 Tg/a (30). Also, India and China's dominance in livestock-emissions (23) and S.E. Asian rice cultivation are consistent with the location of the source increase (13)."

We inserted in the paragraph before:
"Schaefer at al. (2016) by means of 13C/ 12C (CH4) data and a box model concluded that fossil fuel related emissions are a minor contributor to the renewed methane increase, compared to agricultural emissions dominated by ruminants."

Introduction, line 77: "Further, it was concluded that fossil fuel related sources had decreased". It should be stated explicitly who concluded this (it is not clear if this refers only to the [Schwietzke et al., 2016] or to both papers discussed here).
We updated this paragraph:
"As mentioned above, Schaefer et al. (2016) showed that "after 2006, the activation of biogenic emissions caused the renewed CH_4 rise", raising concern about the contribution from rice production versus wetland emissions, and Schwietzke et al. (2016), based on reassessment of data of the $^{13}C/^{12}C$ ratio of CH_4 from fossil sources, conclude that the assumed global fossil fuel CH_4 emissions need a major upward revision of 60-110 %. In other words, it was found by both authors that the combined fossil CH_4 sources (1985-2002) must have been much stronger (factor of 2), at the expense of microbial sources. Further, it was concluded that fossil fuel related sources had decreased."

Model Setup, lines 117-118: "...operational analysis data of the European Centre for Medium-range Weather Forecasting (ECMWF) (van Aalst et al., 2004).": Why did the authors use operational analysis data and not the reanalysis (which should be superior in terms of consistency over time, which is essential for any trend analysis)?
Following the referee's advice, we use the ERA-Interim coefficients in the new simulation.
Reference:
Dee, D. P., et al.: The ERA-Interim reanalysis: configuration and performance of the data assimilation system, Q. J. Roy. Meteor. Soc., 137, 553–597, doi:10.1002/qj.828, 2011.

Model Setup, lines 119-122: " the nudging method is applied in the free troposphere, tapering off towards the surface and tropopause, so that stratospheric dynamics are calculated freely, and possible inconsistencies between the boundary layer representations of the ECMWF and ECHAM models are avoided.": This might be an advantage in terms of self-consistency of the model physics, but may lead to deficiencies to simulate the synoptic-scale variability also in the boundary layer. As outlined in my general comment (2), the capability to simulate the synoptic-scale variations observed at the surface stations needs to be further analyzed (as this is essential to properly simulate the coastal stations used in this study).
see above - and no coastal stations anymore except CGO which is simulated at $R^2 = .93$ (Fig. 1 at the end of this document)

Model Setup, line 127: "photolysis": Is this relevant in the EMAC model domain?
Because the model domain reaches up to 1 Pa we mentioned that for completeness, even the effect is small. "Removal of CH4 by photolysis becomes important only in the mesosphere."
(T. Röckmann et al., The isotopic composition of methane in the stratosphere:

high-altitude balloon sample measurements, Atmos. Chem. Phys., 11, 13287–13304, 2011 doi:10.5194/acp-11-13287-2011)

Model Setup, lines 146-147: "Natural wetland emissions are based on Walter et al. (2000) and Fung et al. (1991).": These are different wetland inventories - which one has been used in this study ? Furthermore, the Walter et al. (2000) reference is missing.

We updated this paragraph:

"Natural wetland emissions are based on Walter et al. (2000), fossil sources based on EDGARV2.0 and remaining sources as compiled by I. Fung et al. (1991)."

Model Setup, lines 153: "GFED statistics": The specific GFED version number should be mentioned.

The new simulation is based on GFEDv4s.

Reference: Randerson, J. T., G.R. van der Werf, L. Giglio, G.J. Collatz, and P.S. Kasibhatla. 2018. Global Fire Emissions Database, Version 4, (GFEDv4). ORNL DAAC, Oak Ridge, Tennessee, USA. https://doi.org/10.3334/ORNLDAAC/1293

Model Setup, lines 154: "EDGAR2.0 database (Olivier, 2001)": Why has this old version of the EDGAR database been used, and not more recent versions?

We did not update this dataset because this category contributes just 2.6 % of total CH4 and because the dataset serves as a priory assumption for the optimization procedure.

Model Setup, lines 161: "yearly differences in the 20 Tg/y biomass burning": I would suggest to replace "yearly" by e.g. "inter-annual".

We follow the referee's suggestion.

Model Setup, lines 179-180, "The negative flux distribution has a pronounced seasonal cycle in phase with the emissions": which emissions are meant here?

In the new simulation the "negative flux" approach is replaced by a "deposition velocity" parametrization which was not yet ready for the old paper version.

We updated the respective paragraph:

"The MESSy sub-model "DDEP" simulates dry deposition of gas phase tracers and aerosols (Kerkweg et al. 2006). For our CH_4 budget modeling the deposition velocity was derived for a fixed atmospheric-methane mixing ratio of 1800 nmole/mole (Spahni R. et al., 2011, Ridgwell et al., 1999) and is scaled correspondingly. The deposition has a pronounced seasonal cycle in phase with the wetland emissions and depends on soil temperature, moisture content and the land cultivation fraction and varies from 2.4 Tg in January to 4.0 Tg in July."

Observations used for model verification, line 190: Maybe replace "verification" by "validation" (however, there is indeed not a consistent use of these terms in the scientific literature)

We follow the referee's suggestion.

Observations used for model verification, lines 199-205: The calibration scales used should be mentioned, including potential differences between the NOAA and AGAGE scales.

NOAA standard scale (Dlugokencky et al., 2005)

ALE/GAGE calibration procedure (Prinn et al., 2000)

Observations used for model verification, lines 199-205: Why has only this very limited set of atmospheric stations been used (see general comment (1))?

As mentioned above, now 16 NOAA stations

Observations used for model verification, lines 205-207: "Monthly mean mixing - unfiltered with respect to local pollution events - are compared to respective monthly averaged model samples...": Why did the authors use monthly mean values, and not hourly or daily averages (see general comment (2)) ?

As mentioned above, consistently with the measurements, the model now samples at every time step and averages at the end of every month (sub-model SCOUT).

In consideration of the 20 year's simulation period and the >8 years lifetime of methane are comparing monthly means.

Observations used for model verification, lines 209ff: which calibration scale has been used for the CARIBIC CH4 measurements?

We inserted:

"The calibration is carried out using NOAA Methane WMO scale (Dlugokencky et al., 2005) For further information . . ."

►

Simulation results, lines 229-230, "spin-up simulations and scaled to match the 1997 station measurements", and lines 254-255 " For initialization, a global methane distribution pattern for January was created iteratively in several and finally rescaled to Jan. 1997 station measurement data": The spin-up and scaling should be described in more detail (but best in section with model description): how long is the spin-up, which emissions have been used (probably the same as for the period 1997-2006?)? Did you just scale the calculated 3D fields?

We introduced in

Ch. 2, Model Setup:

"Using a priori emission estimates, an initial CH_4 distribution was derived in the course of several spin-up simulations repeated until a steady state global CH_4 mass has settled over the years 1997 through 2006."

Ch. 2.2.1 Methane emissions:

"The GFED biomass burning statistics include agricultural waste burning events. Biomass burning emissions are inter-annually variable and the 1997 emission was 2.4 times as high as the 1998-2015 average (Fig. S1c)."

4.1 The period 1997 through 2006

"For initialization, a global methane distribution pattern for January was created as mentioned above and ensures a balanced annual average global CH_4 mass over the entire period with inter-annually constant sources and sinks up to deviations caused by variations in biomass burning."

Ch. 4.1.1 NOAA/AGAGE stations

"The initial distribution, which is the result of a long term simulation, does not precisely reflect the special Jan. 1997 situation, but obviously overestimated starting values at northern hemispheric stations level down in the course of the first six months. The Solver cannot improve this because it acts on the whole biomass burning series and not on individual years."

If so, there would be some inconsistency between the applied emissions and the concentrations (which may also explain why the simulated CH4 concentrations still increase between 1997 and 2000).

Figs. 1 and 5 in the new paper version (cf. Fig. 1 for CGO at the end of this document) reveal an increase also in the between 1997 and 2000. NH-enhanced values level down within six months and are caused by the anomaly in GFED biomass burning.

Simulation results, lines 265-269: "The linear dependency between source strength and atmospheric abundance...", and lines 286-289: "The integrated model CH4 masses exactly match the mass calculated": this has already been discussed before.

New formulation:

"The linear dependency between source strength and atmospheric abundance is reflected in the model's partial differential equation system and allows the redistribution . . ."

Simulation results, line 310: "... fossil group of categories comprising landfill-, coal-, gas-, and oil (FOS)": CH4 from landfills are (usually) not fossil, but primarily from relatively recent carbon.

In the new simulation that is no longer an issue: all categories are considered individually.

Simulation results, line 346: "In contrast to the monthly average station data, the CARIBIC individual methane observations...": The station data - as provided to users - are hourly data. See also general comment (2).

The usage of the sub-model SCOUT, consistently with the measurements, samples at every time step and averages at the end of every month.

Simulation results, lines 365-366: "...suggesting that the vertical resolution of the model grid is not optimal to resolve the fine structure in the tropopause region.": Probably this is not only due to coarse vertical resolution, but also due the vertical CH4 gradient in the stratosphere.

The comment of the referee is not in contradiction to our conclusion: The tropopause region with the declining vertical CH4 gradient cannot be properly resolved due to the course vertical resolution (~500m) of the hybrid model grid at this altitude.

Simulation results, line 369: "according to the definition in Sect. 3.2 (Fig. S3)..." I assume this should be Fig. S2?
According to the referees comment, in the updated version, Fig. S3 now is correctly referred as Fig. 2b

Simulation results, lines 386-387: "Figs. 12a and b...logarithmically scaled": the figures seem so use a linear scale. Furthermore, the figures show concentrations, while the figure caption states "Assumed additional emissions..." (Should be rephrased to e.g. "Impact of assumed additional emissions...").
According to the referees comment Fig. 12 is now Fig. S2 in the updated version and log scaled. We rephrased to "Impact of assumed additional emissions . . ."

Simulation results, lines 391-392: "...upper estimate from Bergamaschi et al. (2013) of 22 Tg CH4 yr-1 as a first guess": It should be mentioned that the estimate of Bergamaschi et al. (2013) is for a different time period (2007-2010), compared to the 2007-2014 period used in this study.
Following the referee's advice we avoid a citation because the 28 Tg CH4/y in the new version this has to be considered just as an upper limit for the Solver:
"We used an upper limit emission of 28 Tg CH_4/yr to be added in order to fit the upward trend."

Simulation results, lines 395-396: "Both scenarios perfectly reproduce the observed CH4 trend...": I would suggest to avoid the term "perfectly".
We avoided the term "perfectly".

Simulation results, lines 400-401: "Changes in the removal rate of methane by the OH radical have not been seen in other tracers of atmospheric chemistry, e.g. methyl chloroform (CH3CCl3) (Montzka et al., 2011; Lelieveld et al. 2016) and do not appear to explain short-term variations in methane.": I do not agree with this statement. Although Montzka et al. [2011] derive only small interannual variability their CH3CCl3 based estimates still show variations on the order of +/- 3%, which is equivalent to a variability of the OH sink of +/- 17 Tg CH4 yr-1. Furthermore, the recent papers of and Turner et al. [2017] demonstrated the potential significant impact of variations in OH on the trend and inter-annual variability of CH4. I suggest to include the references to the two papers.
Following the referee's advice we refer to Turner et al. (2017) in the new text. :
"Turner et al. (2017) based on numerical analyses find that a combination of decreasing methane emissions overlaid by a simultaneous reduction in OH concentration (the primary sink) could have caused the renewed growth in atmospheric methane. However they cannot exclude rising methane emissions under time invariant OH concentrations as a consistent solution to fit the (rising) observations."

Simulation results, lines 423-424: "This shows that, when the SHA emissions are located away from the North America, no fraction is found that could minimize simultaneously the _NS and RMS": Given the very limited number of stations (see general comment (1)) and the question how well coastal / regional stations are simulated by the EMAC model (see general comment (2)), the question is, if this finding is really significant / robust.

The new simulation now considers 16 stations– and optimization procedure upgraded

Simulation results, line 437: "linear trend lines 0.32x (CARIBIC) and 0.31x (EMAC)": units are missing

New formulation:

"The slopes of the linear trend lines 0.32x (CARIBIC) and 0.31x (EMAC) over time where x = number of months . . ."

Simulation results, lines 451-452: "the tropopause influence is stronger": probably also the influence of the lower stratosphere.

New formulation:

"the influence of the lower stratosphere is stronger, leading to reduced linear slopes together with comparably less R^2 of 0.59 and 0.72 (Fig. 14). "

Conclusions and Outlook, lines 488-496: Would be useful to expand the conclusions, including a discussion / summary of the novel aspects of this study, the uncertainties of the results and limitations of the study. Furthermore, it should be summarized, how the results from this study compare with the existing literature studies.

A co-author is taking care for this and his findings will be incorporated in the conclusions as soon as possible.

Conclusions and Outlook, lines 497-499: "In view of the additional global CH4 source since 2007, a source – sink equilibrium has not yet established after the 8 years of emissions considered. A 2nd order polynomial extrapolation predicts steady state after 13 years, assuming that the emissions remain unchanged.": This scenario seems quite hypothetical, and global emissions (including their latitudinal distribution) remaining constant over 13 years relatively unlikely.

Following the referee's advice we included in

***4.2 Simulating the recent methane trend** - first paragraph:*

"Between 2007 and 2013 the slope appears nearly linear (Fig. 1), and the discrepancy can be removed by assuming an additional constant CH_4 source for this period. We find that after 2013 an additional increment is necessary to fit the trend."

and in

5 Conclusions and Outlook:

"A 2nd order polynomial extrapolation predicts steady state after 13 years, assuming that the emissions remain unchanged, which does not seem realistic in view of the observed development after 2013/14 (Fig. 1). "

Conclusions and Outlook, lines 497-499: "Nevertheless, the degree of freedom in the

choice of sources is limited,...": Taking into account also uncertainties in the spatial (and temporal) distribution of emissions, a very large number of emission scenarios is possible - while only 2 scenarios were investigated in this study (see gen. com. (3)).

Following the referees comment we formulated:

"Two possible additional methane sources, shale gas extraction (SHA) and tropical wetlands (TRO) have been investigated, that could cause the resuming methane growth since 2007. We showed that a methane increase of 25.47 Tg/y in 2007 and subsequent years, of which 69 % from TRO and 20 % from SHA, can optimally explain the recent CH_4 trend until 2013."

As mentioned above, realizing a significant underestimation from 2007 on, just the two hypothetical scenarios TRO and SHA have been included for sensitivity testing of the observed trend.

Table 1: references should be given for the individual a priori emission estimates.

The methane emissions are based on (Houweling et al. 2006)

The "burning"-part of the GAMeS dataset is replaced by the GFEDv4s statistics (Randerson et al., 2018) in addition to biofuel combustion emissions from the EDGAR2.0 database (Olivier, 2001).

Figures - general comment: The number of figures seems very large - several of them could be put in the supplementary material.
Following the referees comment we reduced the number of figures.

Figure 1: How were the data fitted?
The data have been fit by linear regression – now formula inserted for better interpretation.

Figure 3: Explain the meaning of the individual red circles
Figure no longer used

Figure 4a: "Zero" point (a priori emissions) should be indicated
Figure no longer used because of non-linear Solver approximation in the new version.

Figure 4b: What is the meaning of the curves (interpolation) between the individual stations?
In the new version "Figure 3 at the end of this document" includes 16 stations and interpolating lines left out.

Figure 5: "dashed line": The figures seem not to show any dashed line.
"dashed line": Text updated.

Figure 7: What is the meaning of the colors?
now "Figure S6" no more color shift

Figure 11b: Is the shown average for all CARIBC flights as function of time really very useful? Probably the spatial coverage of the flights is also changing significantly over time.
It turned out to be useful, because in the beginning we were misguided by some Africa flights in a way that we tended to blame to low model mixing ratios to convection problems. This graph finally demonstrated the methane increase and the effect on Africa flights which started in 2009.

Figure 13b: What is the meaning of the curves (interpolation) between the individual stations?
In the new version "Figure 10" includes 16 stations - interpolating lines in this graph are helpful to visually associate the points to a category. (cf. Fig. 4 at the end of this document)

Figure 16: (as for Figure 11b): How is the spatial coverage of the flights changing over time?
The spatial coverage of the flights changing over time used to be depicted in Fig.S6, which is now Fig. S7 in the new paper version.

Figure 17: Legend needs to be explained. Which curves are for which period?

Fig. 17 is now Fig. 15 in the new version and the legend is updated (cf. Fig. 15copy at the end of this document).

References

Dlugokencky, E. J., L. Bruhwiler, J. W. C. White, L. K. Emmons, P. C. Novelli, S. A. Montzka, K. A. Masarie, P. M. Lang, A. M. Crotwell, J. B. Miller, and L. V. Gatti, Observational constraints on recent increases in the atmospheric CH4 burden, Geophys. Res. Lett., 36(L18803), doi: 10.1029/2009GL039780, 2009.

Dlugokencky, E. J., E. G. Nisbet, R. Fisher, and D. Lowry, Global atmospheric methane: budget, changes and dangers, Phil. Trans. R. Soc. A 369(1943), 2058-2072, doi: 10.1098/rsta.2010.0341, 2011.

Rigby, M., R. G. Prinn, P. J. Fraser, P. G. Simmonds, R. L. Langenfelds, J. Huang, D. M. Cunnold, L. P. Steele, P. B. Krummel, R. F. Weiss, S. O'Doherty, P. K. Salameh, H. J. Wang, C. M. Harth, J. Mühle, and L. W. Porter, Renewed growth of atmospheric methane, Geophys. Res. Lett., 35(L22805), doi:10.1029/2008GL036037, 2008.

Rigby, M., S. A. Montzka, R. G. Prinn, J. W. C. White, D. Young, S. O'Doherty, M. F. Lunt, A. L. Ganesan, A. J. Manning, P. G. Simmonds, P. K. Salameh, C. M. Harth, J. Mühle, R. F. Weiss, P. J. Fraser, L. P. Steele, P. B. Krummel, A. McCulloch, and S. Park, Role of atmospheric oxidation in recent methane growth, Proceedings of the National Academy of Sciences, 114(21), 5373-5377, doi: 10.1073/pnas.1616426114, 2017.

Saunois, M., P. Bousquet, B. Poulter, et al., Variability and quasi-decadal changes in the methane budget over the period 2000–2012, Atmos. Chem. Phys., 17(18), 11135-11161, doi: 10.5194/acp-17-11135-2017, 2017.

Schaefer, H., S. E. Mikaloff Fletcher, C. Veidt, K. R. Lassey, G. W. Brailsford, T. M. Bromley, E. J. Dlugokencky, S. E. Michel, J. B. Miller, I. Levin, D. C. Lowe, R. J. Martin, B. H. Vaughn, and J. W. C. White, A 21st century shift from fossil-fuel to biogenic methane emissions indicated by 13CH4, Science, doi: 10.1126/science.aad2705, 2016.

Turner, A. J., C. Frankenberg, P. O.Wennberg, and D. J. Jacob, Ambiguity in the causes for decadal trends in atmospheric methane and hydroxyl, Proceedings of the National Academy of Sciences, 114(21), 5367-5372, doi: 10.1073/pnas.1616020114, 2017.

Worden, J. R., A. A. Bloom, S. Pandey, Z. Jiang, H. M. Worden, T. W. Walker, S. Houweling, and T. Röckmann, Reduced biomass burning emissions reconcile conflicting estimates of the post-2006 atmospheric methane budget, Nature Communications, 8(1), 2227, doi: 10.1038/s41467-017-02246-0, 2017.

2018.

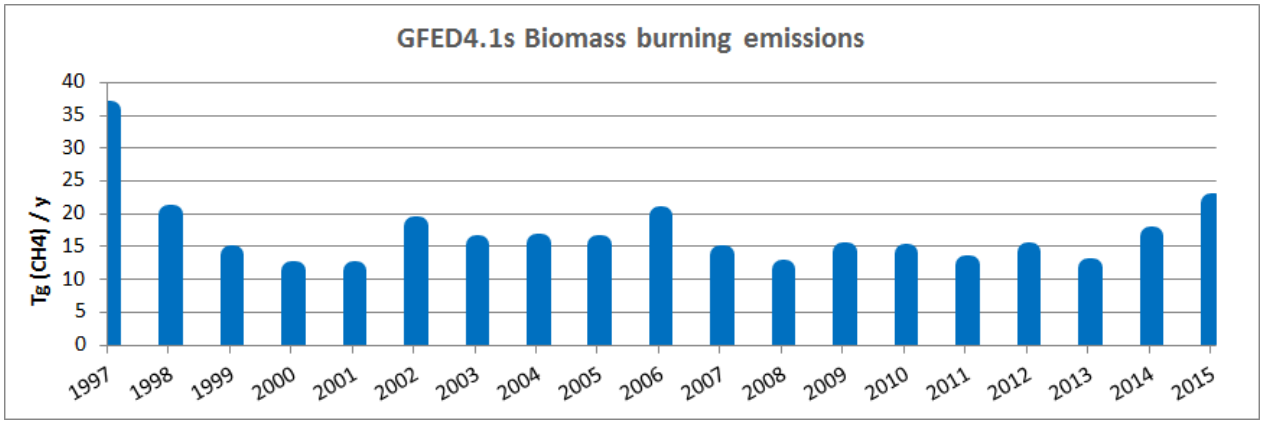

Figure 1: The integrated annual amount was calculated 5.7e12 g higher by the solver.

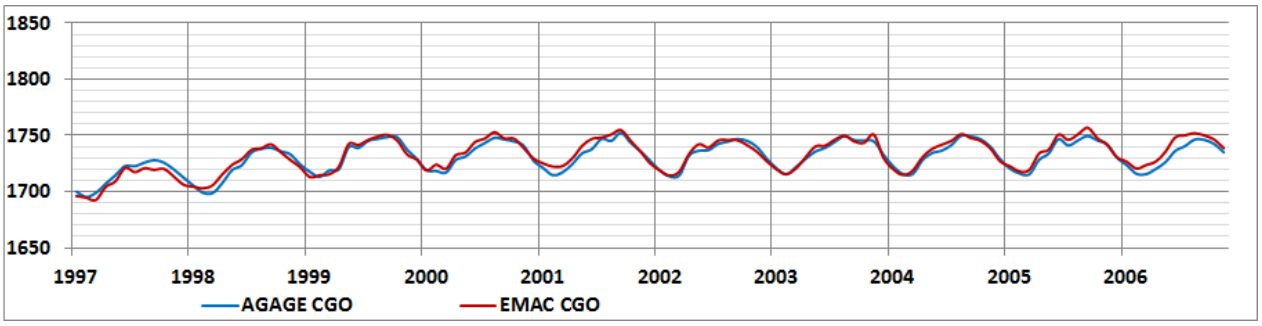

Figure 2: AGAGE station CGO, Cape Grim, Tasmania:
Observations (blue) vs simulation (red) – R^2 = .93

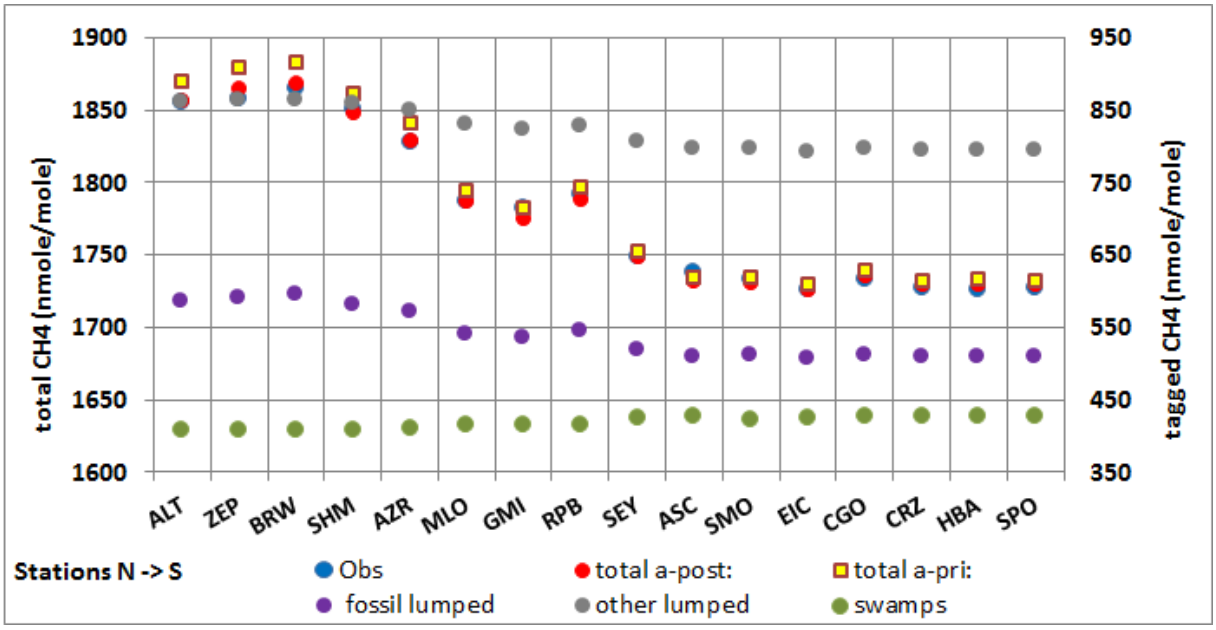

Figure 3: Optimization of calculated ground station CH4 mixing-ratios towards observation (blue) in north-south direction by scaling the tagged emission contributions (now Fig. 6 in paper).

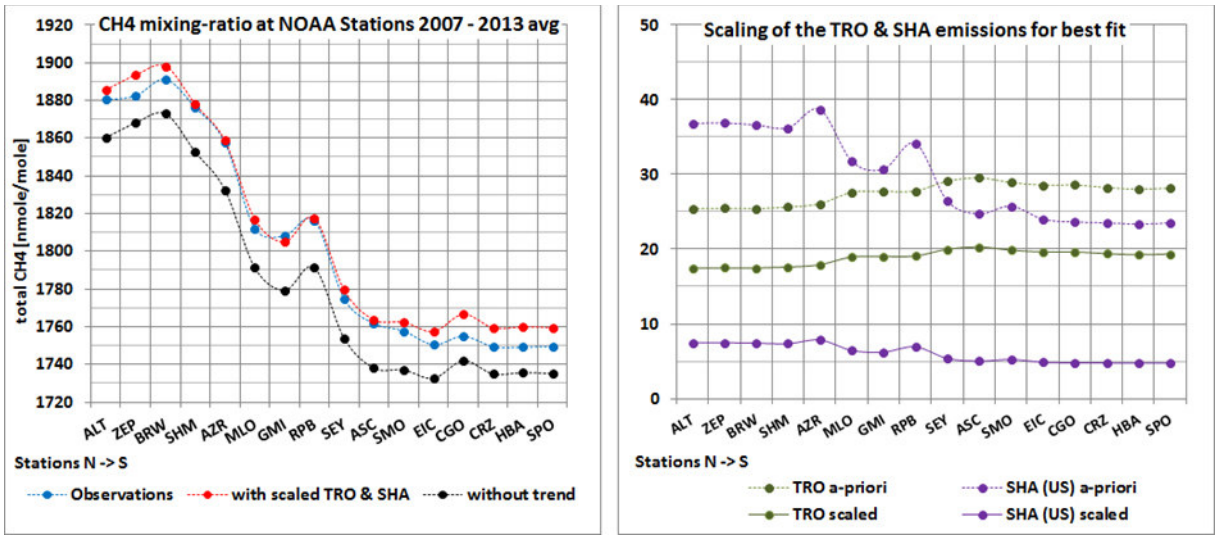

Figure 4: Scaling TRO and SHA emission fractions to fit the all-station observations within smallest RMS:
Left: Observations (blue) and total calculated CH4 without- (black), and with (red) trend period emissions (solid lines right panel).
Right: A-priori estimates (dashed) and solver-scaled (solid) TRO (19.44)- and SHA (5.74 Tg/y) emissions for trend years. (now Fig. 10 in paper).

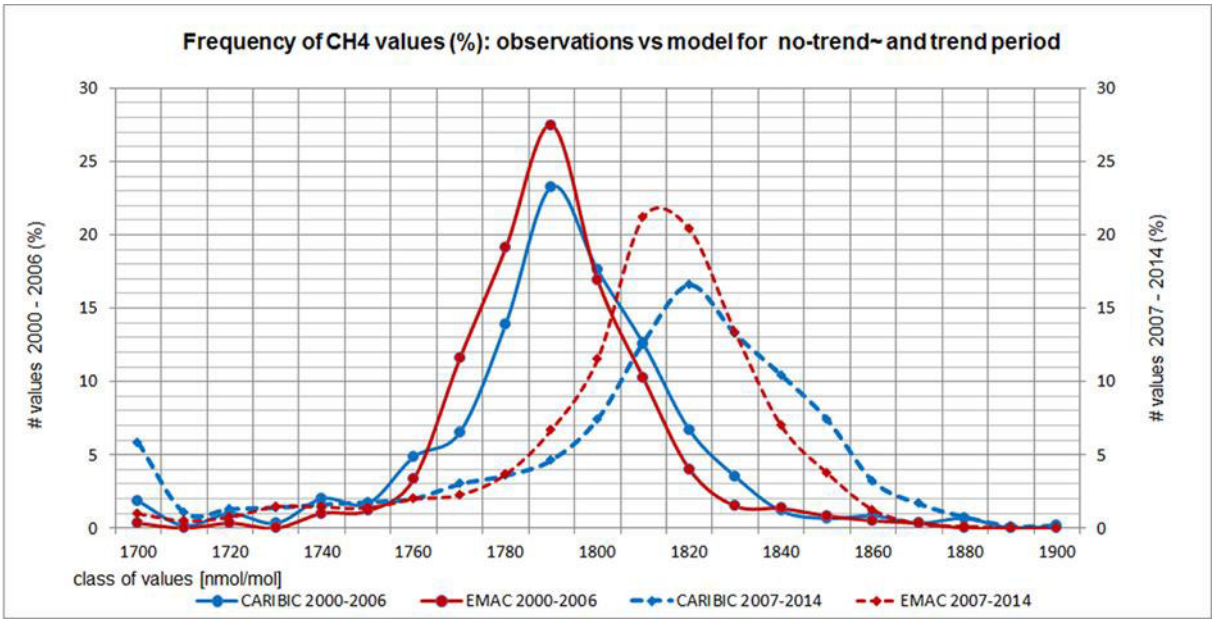

Figure 15copy: Frequency spectrum of CARIBIC observed and EMAC simulated CH4-mixing-ratios separately plotted for the years 2000-2006 and 2007-2014.

We thank the referee for the comments.
Here the comments are listed with our reply.

General Comments

The authors should really explain how the selection of stations was made. It is even stated in the title that they use NOAA stations for methane, but only the Mauna Loa Observatory is used. Also the number of stations seems quite limited to accurately represent the global methane.

Indeed only a limited amount of stations were used in the comparison. Following the referee's advice, the simulation was repeated using 16 NOAA stations and CGO(AGAGE) :

Code	Station Name	Country	Lat °	Lon °	elevation / m
ALT	Alert	Canada	82.45	-62.51	190
ASC	Ascension Island	UK	-7.97	-14.40	85
AZR	Terceira Ile., Azores	Portugal	38.77	-27.38	19
BRW	Barrow, Alaska	USA	71.32	-156.61	11
CGO	Cape Grim, Tasmania	Australia	-40.68	144.69	94
CRZ	Crozet Island	France	-46.43	51.85	197
EIC	Easter Island	Chile	-27.16	-109.43	47
GMI	Mariana Islands	Guam	13.39	144.66	0
HBA	Halley Station,	Antarctica, UK	-75.61	-26.21	30
MLO	Mauna Loa, Hawaii	USA	19.54	-155.58	3397
RPB	Ragged Point	Barbados	13.17	-59.43	15
SEY	Mahe Island,	Seychelles	-4.68	55.53	2
SHM	Shemya Island, Alaska	USA	52.71	174.13	23
SMO	Tutuila, Am. Samoa	USA	-14.25	-170.56	42
SPO	South Pole	USA	-89.98	-24.80	2810
ZEP	Ny-Alesund, Svalbard	Norway, Sweden	78.91	11.89	474

The choice of meteorological data seems a bit strange. The operational data of ECMWF have changed vertical resolution at least twice within the study period, definitely affecting the height of each level. This must have an impact on the nudged values and the model results. How did you deal with these issues? Did the meteorological data vertical resolution near tropopause match the model vertical resolution? Also a validation of the computed meteorology is missing from the manuscript.

We thank the referee for pointing this out. The new simulations has been performed using the ERA interim data (Dee et al., 2011), which is consistent for the entire simulation period.

Specific Comments

P1 L25: RMS abbreviation used before defining.
Abstract L27: Root Mean Square deviation (RMS)

P4 L153: Which GFED? GFED4s? Clearly state the version.
GFEDv4: Randerson, J.T., G.R. van der Werf, L. Giglio, G.J. Collatz, and P.S. Kasibhatla. 2018. Global Fire Emissions Database, Version 4, (GFEDv4). ORNL DAAC, Oak Ridge, Tennessee, USA. https://doi.org/10.3334/ORNLDAAC/1293

P5 L178: emission flux, the "e" is missing. – this has been corrected in the manuscript.

P7 L231: A higher resolution of sampling should be used for the CARIBIC data. Daily samples for flight data is far too long.

We apologize for the unclear formulation: the model was sampled daily at 12 UTC at the Stations' location, while for comparison with CARIBIC data the highest possible sampling was used (2 min time-step). Nevertheless, in the new simulation also station values are sampled continuously and then averaged monthly for comparison with observations.

"… calculated CH_4 mixing ratios are recorded and stored at all sampling positions and -times at selected (NOAA (Dlugokencky, 2018) and AGAGE (Prinn et al., 2013) observation sites and along the CARIBIC flight tracks"

P8 L297-305: As mentioned in the general comments, 6 stations are not enough to reach definite conclusions.

This has been changed in the largely revised manuscript.

P10 L360-368: Couldn't this be because of the meteo data?

We exchanged the "operational analyses" with ERA interim with the same effect.
However the high altitude mixing-ratios are averaged over ~500 m grid boxes smoothing down the amplitudes.

P11 L418 and P12 L434 and P13 L495 and Fig13b caption: Be consistent when reporting these numbers.

We corrected the caption.

"…For the years 2007 through 2013 it turns out that a total emission of 25.47 Tg CH_4/y composed of 19.44 Tg TRO and 5.74 Tg SHA optimally reduces the RMS to 0.55 % and approximates the observed ΔNH/SH up to 98%. Fig, 10 …"

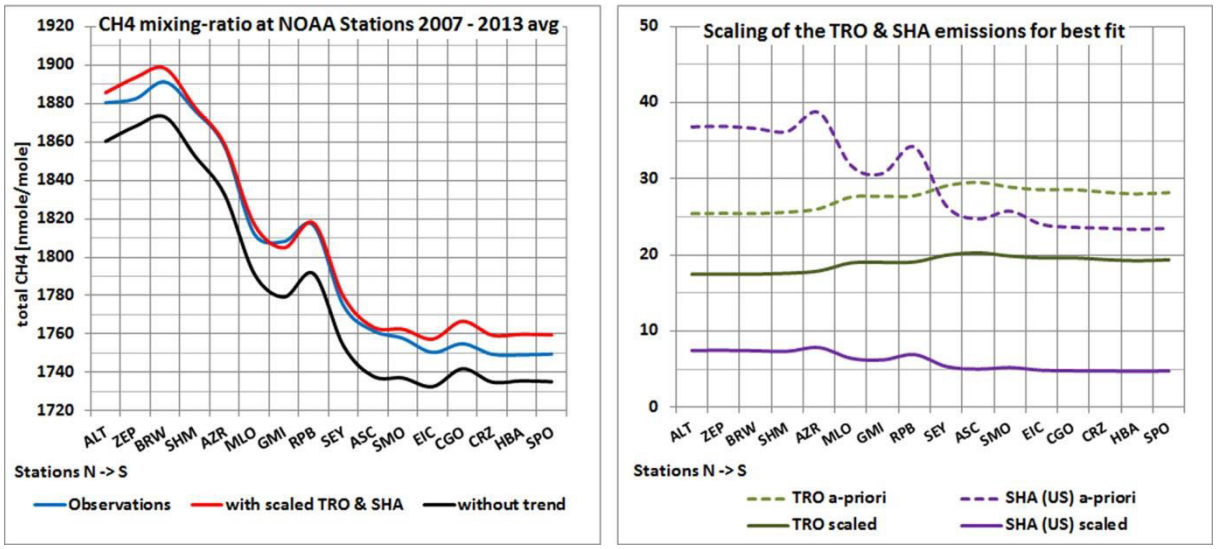

Figure 10: Scaling TRO and SHA emission fractions to fit the all-station observations within smallest RMS: Left: Observations (blue) and total calculated CH_4 without- (black), and with (red) trend period emissions (solid lines right panel).

Right: A-priori estimates (dashed) and solver-scaled (solid) TRO (19.44)- and SHA (5.74 Tg/y) emissions for trend years.

Fig1: A different color code for the different periods would be helpful.

Following referee's suggestion, we change the figure.

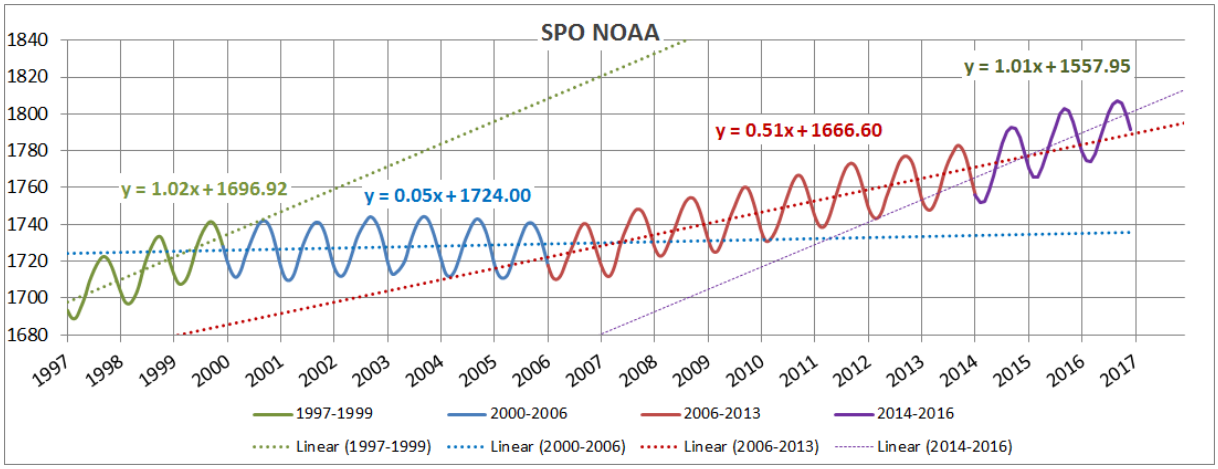

Fig4a and b: I believe the lines connecting the circles are misleading.

New simulation: (I am not sure if looks is better . . . ?)

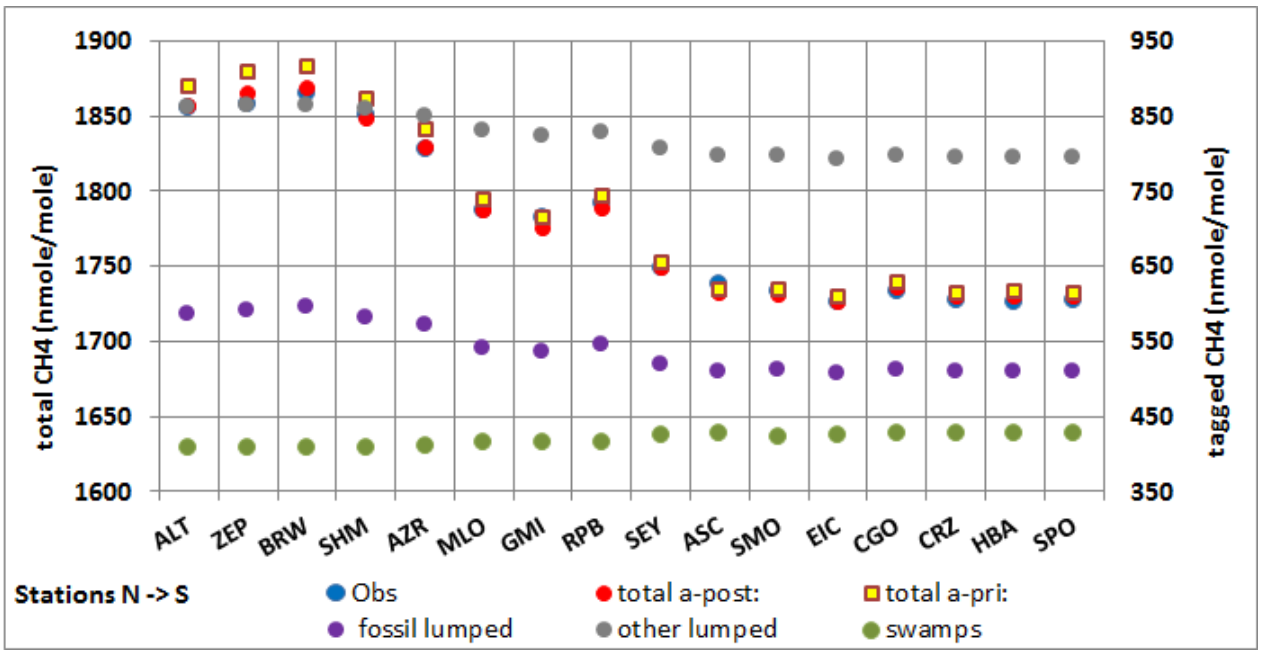

Figs 5, 6, 9, 11, 14, 15: Really hard to read because of size.

Vector graphics of all figures will be provided for the final publication.

Fig13b: again I fail to see the need for the line connecting stations.
New simulation: (I am not sure if looks is better . . . ?)

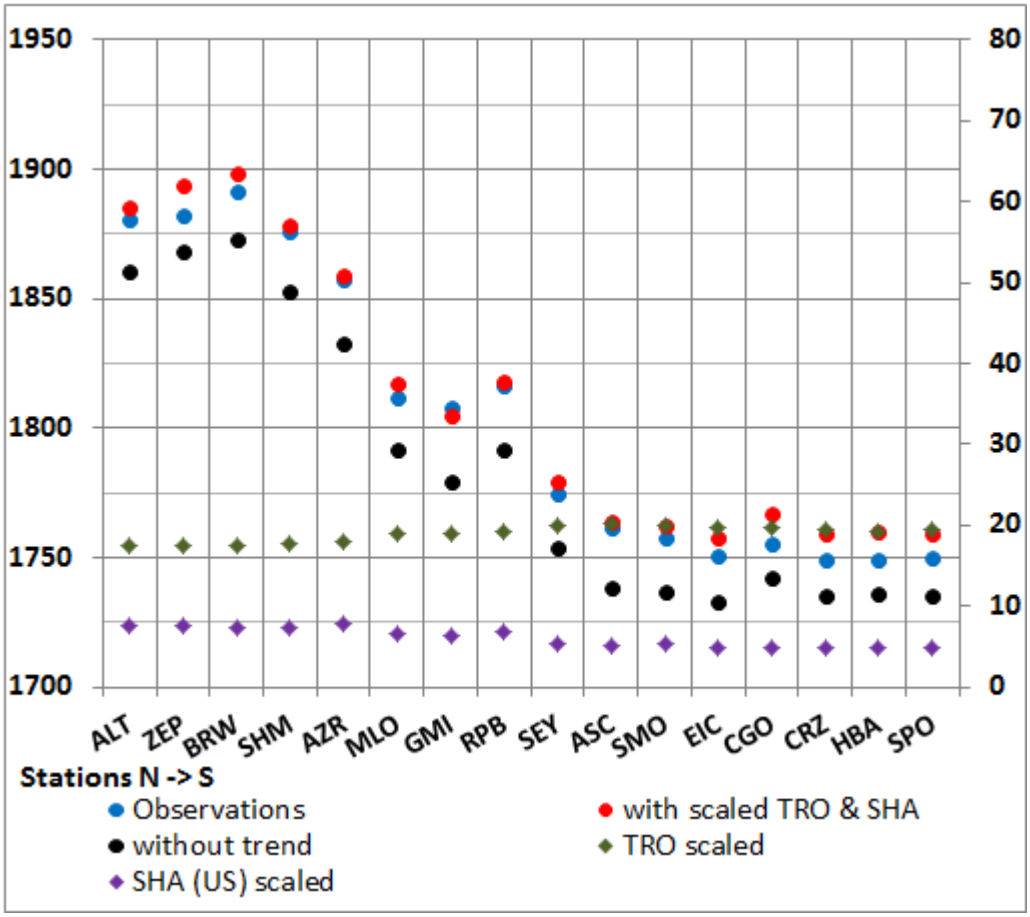

Fig17: State either in the caption or in the legend which set of lines is for every period.
Based on the results of the new simulation, the figure (and caption) has been updated.

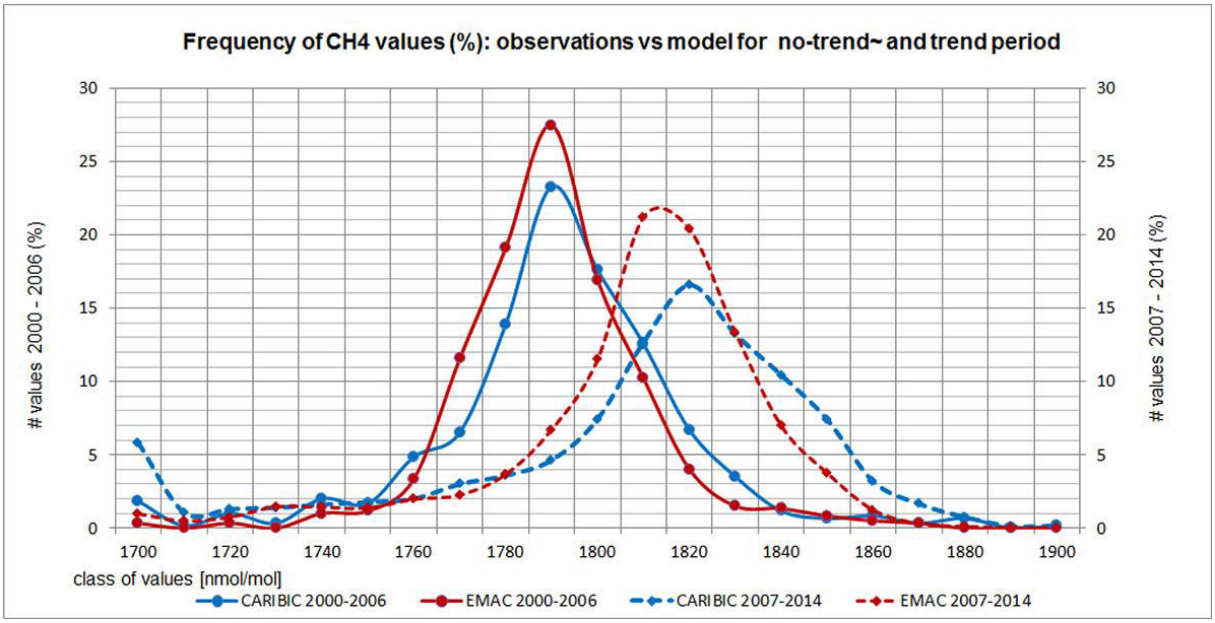

Figure 15: Frequency spectrum of CARIBIC observed and EMAC simulated CH4-mixing-ratios separately plotted for the years 2000-2006 and 2007-2014.

Supplementary material:
There are some inconsistencies between the figures and the captions making it sometimes confusing.
The supplement has been updated.,

Model simulations of atmospheric methane 1997-2016 and their evaluation using NOAA and AGAGE/~~NOAA~~ surface- and IAGOS-CARIBIC aircraft observations~~, 1997-2014~~

Peter H. Zimmermann[1], Carl A. M. Brenninkmeijer[1], Andrea Pozzer[1], Patrick Jöckel[3], Franziska Winterstein[3], Andreas Zahn[2], Sander Houweling[4], and Jos Lelieveld[1]

[1]Max Planck Institute for Chemistry, Department of Atmospheric Chemistry, Mainz, Germany
[2]Karlsruhe Institute of Technology (KIT), Institute for Meteorology and Climate Research, Karlsruhe, Germany
[3] Deutsches Zentrum für Luft- und Raumfahrt (DLR), Institut für Physik der Atmosphaere, Oberpfaffenhofen, Germany
[4] Netherlands Institute for Space Research, Utrecht, the Netherlands

Correspondence to: Peter H. Zimmermann (p.zimmermann@mpic.de)

Abstract.

The global budget, variability and ~~trends~~trend of atmospheric methane (CH_4) have been simulated with the EMAC atmospheric chemistry – general circulation model in specified dynamics mode for the period 1997 through ~~2014~~2016. Observations from seventeen AGAGE and NOAA surface stations and intercontinental CARIBIC flights indicate a transient period of declining methane increase during 1997 through 1999, followed by seven years of stagnation and a sudden resumed increase after 2006.

Starting the simulation with a global methane distribution~~, scaled to match~~ that matches the station measurements in January 1997, and using inter-annually constant CH_4 sources from eleven categories together with photochemical and soil sinks, the model reproduces the CH_4 observations during the transient and constant period from 1997 through 2006 in magnitude as well as seasonal and synoptic variability.

The atmospheric CH_4 ~~calculations~~dry air mole fractions in our model setup without chemical feedback on the reactants are linearly dependent on the source strengths, allowing source segregated simulation of eleven biogenic and fossil emission categories (tagging), with the aim to analyze global ~~CH_4~~ observations and ~~to~~ derive ~~their individual~~ the source specific CH_4 steady state lifetimes~~.~~ (τ). Moreover, tagging enables a-posteriori rescaling of individual emissions with proportional effects on ~~the corresponding inventories and offers a method~~respective source segregated methane abundances. A sophisticated optimization procedure ("Solver") was applied to ~~approximate~~the model results minimizing the ~~station measurements in terms of lowest~~ Root Mean Square deviation (RMS~~. Enhancing the a priori biogenic tropical wetland emissions by ~29 Tg/y, compensated by a reduction of anthropogenic fossil CH_4 emissions,~~) from the observations. Under given constraints the 2000 – 2006 observed all-station mean dry air mole fraction of ~~1792~~1,780 nmol/mol could be ~~simulated~~reproduced within ~~a~~an RMS ~~of~~= 0.~~37 %. The~~ 40 %, associated with a coefficient of determination R^2 = 0.~~87 indicates good agreement with observed variability and the calculated 2000-2005 average~~81. With regard to source optimization this implies a reduction in fossil fuel (predominantly coal and gas) related emissions and an increase in biogenic sources such as tropical wetlands and rice paddies. The observed interhemispheric ~~methane~~ difference between ~~selected NH~~the most northerly and ~~SH~~southerly stations ~~of 119 nmol/mol matches the observations.~~was reproduced within 0.76% .

The CH_4 ~~samples from 95 intercontinental CARIBIC flights for the period 1997-2006 are also accurately simulated by the model, with a 2000-2006 average CH_4 mixing ratio of 1786 nmol/mol, and 65 % of the measured variability being captured. This includes tropospheric and stratospheric data.~~

~~To explain the growth of CH_4~~ increase from 2007 through 2013 ~~in term of sources,~~ started nearly linearly, explained by an additional emission ~~increase~~ of ~~28.3~~20.70 Tg/y CH_4 ~~is needed~~. We ~~explore~~explored the contributions of two potential

causes, one representing natural emissions from wetlands in the tropics "TRO", and the other anthropogenic (e.g. shale gas ~~production~~fracturing) emissions in North America~~.~~ "SHA". Based on the ~~acceptance of the~~a posteriori no-trend period emission distribution ~~a 62.6 % tropical wetland together with a 37.4 % shale gas contribution~~, with the Solver we estimated additional annual 12.30 Tg/y TRO and 8.40 Tg/y SHA contributions, respectively, to optimally ~~fits~~fit the trend~~, and simulates CH_4 from 2007 – 2013 with an~~ (RMS ~~of 7.1 nmol/mol (~~= 0.~~39 %). The coefficient of determination of~~55 % / R^2 = 0.~~91 indicates even better significance than before 2006~~8). After 2013 the trend steepened and required a 2.0 Tg larger increment per year, probably from an additional source in eastern Asia and unchanged tropical and North American sources.

~~The 4287~~Nearly 800 CH_4 samples gathered during 95 intercontinental CARIBIC flights in the upper troposphere and lower stratosphere (UTLS) in the period 1997-2006 were simulated within RMS = 1.1 % deviation from the mean CH_4 mixing ratio, mostly over the Northern Hemisphere. While measurements were quite disperse in time, the relatively continuous India flight record between 1997 and 2001 was reproduced within an RMS = 0.98 % and R^2 = 0.65. Similarly, more than 4,000 samples collected during 232 CARIBIC flights after 2007 ~~are~~were simulated with an RMS = 1.30 %. The coefficient of ~~1.3 % and~~determination R^2 = 0.~~8, indicating~~80 implies that the model reproduces 80 % of the seasonal and synoptic variability of CH_4 in the ~~upper troposphere and lower stratosphere.~~ UTLS. The slope of the linear regression analysis with 0.58 however indicates evident underestimation of the calculated CH_4 variability because the vertical resolution of the model grid is not sufficient to resolve the fine structure in the tropopause region.

1 Introduction

The greenhouse gas methane (CH_4) is emitted into the atmosphere by various natural and anthropogenic sources, and is removed by photochemical reactions and to a small extent ~~by soils.~~through oxidation by methanotrophic bacteria in soils (Dlugokencky et al., 2011). The tropospheric mean lifetime of CH_4 due to oxidation by OH has been estimated to be 8-9 years (Lelieveld et al., 2016) and its concentration has been growing by about 1 %/y since the beginning of the Anthropocene in the 19th century (Crutzen, 2002, Clais et al. 2013).

The resulting factor of 2.5 ~~fold~~ increase ~~of~~in the global ~~CH_4~~ abundance of atmospheric methane (CH_4) since ~~pre-industrial times produces a climate forcing of~~ 1750 contributes 0.~~57~~5 Wm^{-2} ~~(~~to total direct ~~0.44Wm^{-2}, indirect 0.13Wm^{-2}) which is about 35 % of the climate~~radiative forcing by ~~CO_2 (1.6Wm^{-2}~~long-lived greenhouse gases (2.8 Wm^{-2} in 2009), while its role in atmospheric chemistry adds another approximately 0.2~~) (Lelieveld et al., 1998;~~ Wm^{-2} of indirect forcing (Dlugokencky et al., 2011). ~~In~~ Etminan et al. (2016) presented new calculations including the impact of the ~~IPCC fifth report an even higher~~ shortwave forcing ~~of 0.97 Wm^{-2} corresponding to about 57 % of~~and found that the ~~climate~~1750–2011 radiative forcing ~~by CO_2 (1.68Wm~~is about 25% higher (increasing from 0.5 Wm^{-2}~~) is assessed (IPCC,~~ to 0.6 Wm^{-2}) compared to the value in the Intergovernmental Panel on Climate Change (IPCC) 2013~~).~~ assessment. After the strong upward CH_4 trend since the 1960s, by the end of the 1990s the increase had slowed down until sources and sinks quasi balanced for about 8 years, while in 2007 the CH_4 increase resumed unexpectedly (Bergamaschi et al., 2013). Fig. 1 demonstrates the development of the CH_4-mixing ratio at the ~~AGAGE~~NOAA observation site ~~Cape Grim, Australia (41°~~South Pole (SPO, 90° S~~, 145° E~~) over the years 1997 through ~~2014~~2016, the period considered in this modeling study, and ~~reveal~~reveals a no-trend period from 2000 through 2006.

The resuming upward trend after 2007 (Dlugokencky et al., 2009; Rigby et al., 2008, IPCC 2014) is not fully understood: data analysis (Nisbet et al., ~~2014~~2016, Worden et al., 2017) and inverse modelling studies (Bergamaschi et

al., 2013) indicate that global emissions since 2007 were about 15 to ~~22~~25 Tg CH_4/y higher than in previous years, possibly caused by increasing tropical wetland emissions and anthropogenic pollution in mid-latitudes of the northern hemisphere. A potentially growing source that was identified is hydraulic shale gas fracturing, for instance in Utah, where 6 to 12 % of the natural gas produced may locally leak to the atmosphere (Karion et al., 2013, Helmig et al. 2016). The increasing production of fossil fuels to some extend may ~~thus~~ explain the CH_4 trend~~, but following Nisbet et al., (2014), although this inference needs to be reconciled with observations of ^{13}C in methane, as it was found that since 2007 atmospheric methane had become more strongly depleted in ^{13}C, being an indication that the upward trend is dominated by the ^{13}C depleted biogenic wetland and ruminant emissions.~~; however, Schaefer at al. (2016) by means of ^{13}C/ ^{12}C (CH_4) data and a box model concluded that fossil fuel related emissions are a minor contributor to the renewed methane increase~~.~~, compared to agricultural emissions dominated by ruminants. Simultaneously, "since 2007 $\delta^{13}C$-CH_4 (a measure of the $^{13}C/^{12}C$ isotope ratio in methane) has shifted to significantly more negative values suggesting that the methane rise was dominated by increases in biogenic methane emissions, particularly in the tropics, for example, from expansion of tropical wetlands in years with strongly positive rainfall anomalies or emissions from increased agricultural sources such as ruminants and rice paddies(Nisbet et al., 2016)."

The causes of the trend changes have been subject of a number of studies, some with contradictory results (for instance, Simpson et al., 2012, and Kai et al., 2012) highlighting the complexity of the processes that control the methane budget during this part of the Anthropocene, combined with a paucity of data.

~~More recently~~As mentioned above, Schaefer et al. (2016) showed ~~by means of $^{13}C/^{12}C(CH_4)$ data and a box model~~ that "after 2006, the activation of biogenic emissions caused the renewed ~~[~~CH_4~~]~~ rise", raising concern about the contribution from rice production versus wetland emissions, and Schwietzke et al. (2016), based on reassessment of data of the $^{13}C/^{12}C$ ratio of CH_4 from fossil sources, conclude that the assumed global fossil fuel CH_4 emissions need a major upward revision of 60-110 ~~% .~~%. In other words, it was found by both authors that the combined fossil CH_4 sources (1985-2002) must have been much stronger (factor of 2), at the expense of microbial sources. Further, it was concluded that fossil fuel related sources had decreased. Although the findings of the two articles are not necessarily in conflict, their results warrant further work on the methane budget. Hausmann et al. (2016), using methane and ethane column measurements, concluded that the increase in CH_4 since 2007 has been ~~for~~between 18 to 73 % (depending on assumed ethane/methane source ratios) due to thermogenic methane. Further, Helmig et al. (2016) suggested a large contribution of US oil and natural gas production to the increased emissions. Saunois et al. (2016), in an extensive review of the methane budget, conclude that CH_4 emissions from agricultural activities seem to be a major, possibly dominant cause of the atmospheric growth trend of the past decade. This not only puts the focus on biogenic ~~versus~~over thermogenic, but highlights that both source types are directly influenced by human activity, with the option of being controlled by the implementation of policies.

Here we investigate how well, based on source estimates, CH_4 concentrations and their changes over the past two decades can be simulated numerically, by accounting for atmospheric dynamical and chemical processes with the ~~atmospheric chemistry general circulation model EMAC~~ECHAM/MESSy Atmospheric Chemistry (EMAC) , which describes the transport, dispersion, and chemistry of atmospheric trace constituents, and allows the online sampling of calculated mixing ratios in four dimensions, mimicking the sampling by observational systems (Jöckel et al., 2010). To evaluate the simulation results we use CH_4 ~~concentration data~~measurements at surface stations, i.e. data from NOAA (Dlugokencky et al., 2018) and AGAGE (Prinn et al., 2000) and ~~NOAA (Dlugokencky et al., 2016) and~~ CH_4 data collected by the CARIBIC (Civil Aircraft for the Regular observation of the atmosphere Based on an Instrumented Container) passenger aircraft (Brenninkmeijer et al., 2007).

Both measurement data sets (i.e. the surface-station ~~based~~ and the aircraft based) allow a global approach, with each having its characteristic "footprint". The station data are based on regular measurements at fixed coordinates in both hemispheres. ~~The CARIBIC data (Civil Aircraft for the Regular observation of the atmosphere Based on an Instrumented Container)~~The CARIBIC data are based on monthly flight series (nominally 4 sequential long-distance flights) covering large parts of the globe from a Eurocentric perspective.

A summary of all abbreviations is provided in the "Acronyms" table at the end.

2 Model Setup

2.1 The EMAC numerical model

The ~~ECHAM/MESSy Atmospheric Chemistry (~~EMAC~~)~~ model is a chemistry and climate simulation system that includes sub-models describing tropospheric and middle atmosphere processes and their interaction with oceans, land and human influences. The Modular Earth Submodel System (MESSy, www.messy-interface.org) results from an open, multi-institutional project providing a strategy for developing comprehensive Earth System Models (ESMs) with flexible levels of complexity. MESSy describes atmospheric chemistry and meteorological processes in a modular framework, following strict coding standards. The sub-models in EMAC have been coupled to the 5th generation European Centre HAMburg general circulation model (ECHAM5, Röckner et al., 2006), of which the coding has been optimized for this purpose (Jöckel et al~~.~~., 2006, 2010).

The extended EMAC model version 2.50 at T106L90MA resolution was used to simulate the global methane budget. A triangular truncation at wave number 106 for the spectral core of ECHAM5 corresponds to a ~~(~~~~~~1.1°×1.1~~°)~~° horizontal quadratic Gaussian grid spacing near the equator, and 90 levels on a hybrid-pressure grid in the vertical direction span from the Earth's surface to 0.01 hPa pressure altitude (~80km, the middle of uppermost layer). The vertical resolution near the tropopause is about 500 m. Numerical stability criteria require an integration time step of 1-2 min. With regard to model dynamics, we applied a weak "nudging" towards realistic meteorology over the period of interest, more specifically by Newtonian relaxation of four prognostic model variables temperature, divergence, vorticity and the logarithm of surface pressure towards ~~operational analysis~~ERA interim data (Dee et al., 2011) of the European Centre for Medium-range Weather Forecasting (ECMWF~~) (van Aalst et al., 2004~~).

Apart from the prescribed sea surface temperature (SST~~)~~), the sea-ice concentration (SCI), and the nudged surface pressure, the nudging method is applied in the free troposphere only, tapering off towards the surface and the tropopause, so that stratospheric dynamics are calculated freely, and possible inconsistencies between the boundary layer representations of the ECMWF and ECHAM models are avoided. Further, in the free troposphere, the nudging is weak enough to not disturb the self-consistent model physics, while this approach allows a direct comparison of the model output with measurement data (without constraining the model physics), and therefore offers an efficient model evaluation.

The EMAC sub-model collection includes "CH4" (Frank, 2018) which is tailored for stratospheric and tropospheric methane chemistry and solves the ordinary differential equations describing the oxidation of methane by OH, O^1D, Cl and photolysis. The feedback to the hydrological cycle by modification of the specific humidity is optional in CH4 and was switched off in this particular setup for the same reason as applying tropospheric nudging as mentioned above. ~~The water that is produced by methane oxidation is in the used setup not added to the hydrological cycle. This is indeed only relevant in the stratosphere.~~

The sub-models "SCOUT" and "S4D" enable online sampling of model parameters such as tracer mixing ratio at selected observation sites as well as along aircraft measuring flight routes (http://www.messy-interface.org/ "MESSy Submodels" and Jöckel et al., 2010).

2.2 Model setup for Methane budget investigation

As long as the tracers under consideration are not subject to chemical feedback reactions among each other, they can be processed ~~separately.~~like separate tracers. In this manner, atmospheric ~~constituents such as~~ methane can be tagged e.g. by the source category which they derive from and can be simulated individually, while their sum exactly fits the simultaneous total CH_4 calculations. In our particular case, no feedback is affecting the prescribed OH distribution neither in the gross nor in the tagged mode. ~~(cf. CH. 2.2.3).~~(cf. Sec. 2.3.3). The water that is produced by methane oxidation in the used setup was not added to the hydrological cycle because this is only relevant in the stratosphere.

~~The sub-models "TIMEPOS" and "S4D" enable online sampling of model parameters such as tracer mixing ratio at selected observation sites as well as along aircraft measuring flight routes (http://www.messy-interface.org/ "MESSy Submodels" and Jöckel et al., 2010).~~

The sub-models "SCOUT" and "S4D" enable online sampling of model parameters such as tracer mixing ratio at selected observation sites as well as along aircraft measuring flight routes (http://www.messy-interface.org/ "MESSy Submodels" and Jöckel et al., 2010).

Using a priori emission estimates, an initial CH_4 distribution was derived in the course of several spin-up simulations repeated until a steady state global CH_4 mass has settled over the years 1997 through 2006.

The module "Solver" is a spreadsheet optimizer that is bundled with Microsoft Excel (Fylstra et al. 1998) and uses the "Generalized Reduced Gradient method" (GRG) (Lasdon et al. 1978). A "goal function" defined by the user can be optimized under given constraints upon specific parameters.

In this modeling study the Solver is applied to post-process eleven tagged source segregated a priori tracer distributions (CH_4^i, i = 1, … , 11). The Solver calculates scale factors c^i with the aim to minimize the Root Mean Square deviation (RMS) of $\sum (c^i\, CH_4^i)$ from the observations CH_4^O evaluated at selected ground stations. Constraints have to be imposed under plausibility considerations to avoid unrealistic solutions.

2.~~2~~3 Methane sources and sinks

2.~~2~~3.1 Methane emissions

The combined input from eleven inter-annually constant natural and anthropogenic methane source types amounts to 580 $TgCH_4/y$, applied to the simulation period 1997 – ~~2014.~~2016 (Table 1, col. 3).

Anthropogenic and natural methane sources are based on The Global Atmospheric Methane Synthesis (GAMeS), a GAIM/IGBP (http://gaim.unh.edu/) initiative to develop a process-based understanding of the global atmospheric methane budget for use in predicting future atmospheric methane burdens. Emission data for this initiative have been used for the model setup described here. Natural wetland emissions are based on Walter et al. (2000~~)~~), fossil sources based on EDGARV2.0 and remaining sources as compiled by Fung et al. (1991). Processes with similar isotopic characteristics are aggregated into one group. Oil related sources, for example, comprise mining and processing of crude fuel and all emission classes related to the use of fossil fuel such as residential heating, on/offshore traffic, industry, etc., and also ~~includes~~include an estimate of volcanoes (Houweling et al., 1999). Given that methane

emissions from boreal/arctic wetlands are quite uncertain, it is reasonable to assume that this source category accounts for permafrost decomposition emissions as well.

The "burning"-part of the GAMeS dataset is replaced by the ~~GFED~~GFEDv4s statistics (~~van der Werf~~Randerson et al., ~~2017~~2018) in addition to biofuel combustion emissions from the ~~EDGAR2~~EDGARV2.0 database (Olivier, 2001). The biogenic emissions from bogs, rice fields, swamps and biomass burning are subject to seasonal variability ~~(Tab. 1).~~. About 60 % of the total emissions of 580 Tg/y are caused by human activities; the remainder is from natural sources. At northern middle and high latitudes, methane sources predominantly comprise animals (ruminants), bogs, gas and coal production, transmission and use, landfills, and boreal biomass fires. Tropical wetlands (partly in the subtropics) are the world's largest (natural) source of methane together with animals. Minor tropical anthropogenic input is from biofuel combustion. The individual source strengths are partly subject to seasonal variability, and except for ~~yearly~~inter-annual differences in the ~20 Tg/y biomass burning, are assumed to be inter-annually constant in a reference simulation for the full period 1997 through 2014. More illustrative plots are provided in the supplement, such as Fig. ~~2~~S1a,bS1, which depicts the total emission distribution ~~($gCH_4\ m^{-2}$~~ in g (CH_4) /m^2 /month ~~$^{-1}$)~~ for Jan. (a) and Jul. (b), in logarithmic scale for better representation, to illustrate seasonal CH_4 changes.

A rearrangement among the natural wetland and the anthropogenic landfill-, coal-, gas-, and oil contributions by ~~30~~~20 Tg(CH_4)/y (i.e. ~~5~~3.6 % of the total) in favor of ~~the~~biogenic emissions such as low latitude wetlands and rice paddies has been ~~evaluated~~applied retrospectively under the condition of least RMS deviation between station and model CH_4 mixing ratios ~~(Table 1, column 2).~~.

The horizontal resolution of all methane fluxes is 1°×1°. Because biomass burning emissions are associated with thermal uplift, they are vertically distributed up to 3000 m altitude and higher according to a profile suggested in EDGAR3.2ft (Aardenne et al., 2005). The ~~GFED~~GFEDv4 biomass burning statistics include agricultural waste burning events. Biomass burning emissions are inter-annually variable and the 1997 emission was 2.4 times as high as the 1998-2015 average (Fig. S1c).

Additional emission sources are necessary to close the budget during the methane rising period after 2006. The contributions by enhanced release from tropical wetlands ~~(TRO)~~ and North American shale gas drilling ~~(SHA)~~ ~~(~~FracFocus, 2016) are discussed in Sect. 4.2 and displayed in Fig. S2a, b.

2.~~2~~3.2 Methane uptake by soils

A small but significant (6.6 % in this study) removal process of methane is its oxidation by methanotrophic bacteria in soils (Dlugokencky et al., ~~2010). In absence of a well defined~~2011). The MESSy sub-model "DDEP" simulates dry deposition ~~frequency, a negative mission flux of 37.8 Tg (CH_4)/y dependent on season (e.g., 2.4 Tg in January~~ of gas phase tracers and ~~4.0 Tg in July) at~~aerosols (Kerkweg et al. 2006). For our CH_4 budget modeling the ~~surface is applied, based on~~deposition velocity was derived for a fixed atmospheric-methane mixing ratio of 1800 nmol/mol (Spahni R. et al., 2011, Ridgwell et al~~. (~~., 1999~~). The negative flux distribution~~) and is scaled correspondingly. The deposition has a pronounced seasonal cycle in phase with the wetland emissions and depends on soil temperature, moisture content and the land cultivation fraction and varies from 2.4 Tg in January to 4.0 Tg in July.

~~2.~~2.3 Methane chemical removal

The chemical removal process of CH_4 is photo-oxidation, predominantly by hydroxyl (OH) radicals. In addition to the reaction with OH in the troposphere and stratosphere, there are minor oxidation reactions with atomic chlorine (Cl) in the marine boundary layer and the stratosphere and with electronically excited oxygen atoms ($O(^1D)$) in the stratosphere

(Lelieveld et al., 1998; Dlugokencky et al., 2011). In EMAC the methane photolysis and chemical reaction system is numerically solved by the sub-model "CH4". Global distributions of OH, Cl, and O(^{1}D) have been pre-calculated from the model evaluation reference simulation S1 (Jöckel et al., 2006), therefore providing ~~self-~~internally consistent oxidation fields for the model transport and chemistry of precursors. Monthly averaged fields calculated for the year 2000 have been used in this study.

3 Observations used for model ~~verification~~evaluation

The EMAC model simulates the global distribution of methane from given emission source categories, and produces time series of methane distributions as output. Additionally, model samples during the simulation are recorded for the ~~verification~~evaluation of the results at prescribed locations and times. Monthly averaged mixing ratios are computed at the location of selected NOAA and AGAGE~~/NOAA~~ sites and about ~~4600~~4,600 CARIBIC flight measuring samples (Brenninkmeijer et al., 1999, 2007) gathered during more than 350 flights from 1997 through 2014. The station records predominantly serve as a reference for the model- and recursive emission evaluation and help to gain confidence in the CARIBIC flight data analysis and interpretation.

3.1 NOAA and AGAGE ~~and NOAA~~ station network

~~The ALE/GAGE/AGAGE stations are coastal and mountain sites around the world chosen primarily to provide accurate measurements of trace gases with lifetimes that are long compared to global~~ The NOAA Global Greenhouse Gas Reference Network measures the atmospheric ~~circulation times (Prinn et al., 1978, 2013). The AGAGE sites used in~~ distribution and trends of the three main long-term drivers of climate change including methane (CH_4), the subject of this study. The Reference Network is part of NOAA's Earth System Research Laboratory in Boulder, Colorado (https://www.esrl.noaa.gov/gmd/ccgg/~~ are (Fig. S1): Cape Grim, Australia (41° S, 145° E), Cape Mata Tula, American Samoa (14° S, 171° W), Mace Head, Ireland (53° N, 10° W), Ragged Point, Barbados (13° N, 59° W) and Trinidad Head, California (41° N, 124° W), and the NOAA site Mauna Loa, Hawaii, in the United States (19.5°N, 155.6°W, 3397 masl)~~).

The data provided (Dlugokencky et al., ~~2015). In the following we refer to the stations as CGO, SMO, MHD, RPB, THD and MLO, respectively. Monthly mean mixing – unfiltered~~ 2018) are filtered with respect to ~~local~~synoptic scale pollution events~~—~~. We take advantage of 16 stations approximately equally distributed over the globe (Fig. 2a) and remote from the major emission areas to ensure comparability with the model results which are not filtered. For the same reason, in case of Cape Grim, Australia (41° S, 145°) we refer to the unfiltered AGAGE records (Prinn et al., 1978, 2013). At all stations monthly mean mixing-ratios are compared to respective monthly averaged model samples ~~stored every day at 12:00 GMT.~~.

3.2 CARIBIC flight observations

CARIBIC (Civil Aircraft for the Regular Investigation of the Atmosphere Based on an Instrument Container, Brenninkmeijer et al., 2007) is a European~~,~~ passenger aircraft based atmospheric composition monitoring project that has become part of the IAGOS Infrastructure (www.iagos.org). CARIBIC deploys an airfreight container equipped with about 1.5 tons of instruments, connected to a multi-probe air inlet system. The container is installed monthly for 4 sequential measurement flights from and back to Frankfurt or Munich Airport after which air samples, aerosol samples and data are retrieved. The container houses instruments for measuring ozone, carbon monoxide, nitrogen oxides, water

vapor and many more trace gases as well as atmospheric aerosols. Air samples are collected at cruise altitudes between about 10 and 12 km and depending on latitude and season and actual synoptic meteorological conditions represent tropospheric or stratospheric air masses.

Overall the ratio between sampled stratospheric and tropospheric air masses is about 0.5. These air samples are analyzed in the laboratories of the CARIBIC partner community. More than 40 gases are measured including hydrocarbons, halocarbons and greenhouse gases including CH_4. Methane mixing ratios were determined at coordinates along flight tracks over regions such as Europe (EUR), North America (NAM), South America – north (SAN), South America – south (SAS), Africa (AFR), India and Indonesia (IND), and Far East (FAE) and color coded in Fig. ~~S2~~2b. These values, interpolated in time and space onto the model grid, are subject of our evaluation.

The calibration is carried out using NOAA Methane WMO scale (Dlugokencky et al., 2005) For further information about CARIBIC based studies involving CH_4, we refer to Schuck et al. 2012, Baker et al. 2012, and Rauthe-Schöch et al. 2016. For the period 1997-2002, we use data from the first phase of CARIBIC (Brenninkmeijer et al. 1999).

4 Simulation results

Starting with a global distribution derived from spin-up simulations ~~and scaled to match the 1997 station measurements,~~(Sect. 2), a time series of the monthly mean global methane distribution up to December ~~2014~~2016 has been calculated together with ~~daily~~ online samples at ~~AGAGE/NOAA~~the seventeen ground stations and along the CARIBIC flight tracks for comparison. Characteristic features, such as global CH_4 distributions and seasonal cycles as well as the local variability of station and flight records can be successfully reproduced for the first three years 1997 – 1999, during the slowing increase, as well as the subsequent period through 2006 without a trend.

In our specific model setup, the oxidation chemistry, neglecting ~~H_2O~~ chemical feedback~~, and parameterized soil removal process of CH_4 respond~~ reactions on the oxidants as well as on H_2O, responds linearly to the emissions, thus allowing the separate tracer simulation of individual sources by tagging. Consequently, the sum of eleven tagged methane ~~simulations~~tracers exactly ~~reproduces~~reflects the reference ~~CH_4~~ total methane distribution, and the CH_4 composition ~~of methane~~ at any grid point in the atmosphere can be attributed to the specific source categories. ~~Taking advantage of~~Furthermore, the tagging ~~approach, emission sensitivity studies have been performed in order to approximate the ground station observation series within a least square root deviation (RMS).~~

~~Relative to~~retrospectively allows re-scaling the ~~a priori emissions (Table 1, column 2) a 30 Tg CH_4 /y reduction of predominantly northern hemispheric anthropogenic fossil emissions in favor~~source segregated a-priory global methane distributions with the aim of an ~~31 Tg/y increment in natural emissions from tropical wetlands results in a minimum all-station RMS, and accurately reproduces the observed interhemispheric difference between the most northerly and southerly stations.~~ optimal station measurement fitting approach – Sect. 4.1.1.

For the trend period since 2007 we introduced additional emissions, to account for the recent CH_4 increase (Kirschke et al., 2013, Miller et al., 2013, Nisbet et al., ~~2014~~2016, Turner et al., ~~2016).~~2017). Assuming that all methane emissions except those from tropical wetlands remain constant, two hypothetical ~~methane~~ emission scenarios were considered with the aim to explain the discrepancy between observations and the reference simulation from 2007 to ~~2014: TRO, an additional release~~2016. Firstly, we included rising natural CH_4 emissions from tropical wetlands due to enhanced precipitation, and ~~SHA, additional emission~~secondly we implement new fossil emissions from North America based on shale gas drilling statistics. Also for this period the ~~least~~smallest RMS (~~station~~ measurement –vs model ~~simulation~~) deviation is used as a criterion to evaluate the emission scenarios, ~~together with~~and the ~~slopes of the linear regression~~

trends. A linearSolver optimization analysis guidesguided the attribution of a proportionally larger tropical fraction to TRO than to SHA.(Sect. 4.1.1).

4.1 The period 1997 through 2006

For initialization, a global methane distribution pattern for January was created iteratively in several spin-up cyclesas mentioned above (Sect. 2.2) and finally rescaled to Jan. 1997 station measurement data. Because of mass conservation,ensures a realistic initial distribution is important to simulate anbalanced annual average global CH_4 mass that is in steady state over the entire period with inter-annually constant sources and sinks. up to deviations caused by variations in biomass burning. According to prescribed 4-dimensional coordinate tables, calculated CH_4 mixing ratios are recorded and stored at all sampling positions and times at selected (NOAA (Dlugokencky, 2018) and AGAGE (Prinn et al., 2013) and NOAA (Dlugokencky, 2015)) observation sites and along the CARIBIC flight tracks (Brenninkmeijer et al., 1999, 2007) for the years 1997 through 2014 for2016 in view of further graphical and statistical evaluation. Additionally, for the entire time period from 1997 through 2014, based on the mass conserving sources in the EMAC model simulation, for the entire time period a series of global CH_4-distributions was produced and stored in 2-day frequency for statistical and graphical evaluation, together with daily (12:00 GMT) model samples at AGAGE/NOAA stations and along the CARIBIC aircraft flight tracks..

The linear dependency between source strength and atmospheric abundance in this specific model setup (see 2.2) ensures that the sum of all tagged simulationstracers – as mentioned above – is equal to the reference simulationtracer comprising the sum of all emissions. Moreover, this numerical property of the model's partial differential equation system allows the redistribution of certain amounts among – e.g. northern and southern – emitters without affecting the global budget, up to minor effects caused by the sink distribution. .

While the global total CH_4 emissions are relatively well-constrained, estimates of emissions by source category range within a factor of two (Dlugokencky et al. 2011). The global observational networks have shown to be very helpful to derive the emissions at large scales. The CARIBIC observatory provides an additional global view onconstraint of CH_4 abundance and variability in the UTLS, not directly affected by emission sources at the surface, while being sensitive to the vertical exchange of air masses between the lower and upper troposphere.

The use of tagged tracers helps to determine the origin of the methane that is sampled. Tagged initial distributions and tagged soil sinks are calculated as ratios between the respective source fluxes and the total. Corresponding source-segregated CH_4 station and aircraft samples were calculated the same way as infor the reference simulationtracer, but in this case by each category.for all categories. Chemical reactions and photolysis arewere the same for all tagged tracers as in the simulation withfor total CH_4, i.e. the tagged emissions are exposed to the same oxidant environment. Assuming that the sources are inter-annually constant, apart from the variability in the comparably small (3.4 %) biomass burning source, the partial masses of the tagged resultstracers remain in steady state over the simulation period at roughly proportional amounts to the emission fluxes. However, the exact weighting factors, in terms of the steady-state atmospheric lifetimes, vary somewhat around the integral lifetime of$\tau \cong 8.4445$ years (Fig. 3) because of different exposureexposures to the major chemical destruction areas. The individual steady state lifetimes are quantified in ChSect. 4.1.1. and listed in Tab. 1, col. 5).

The integrated modeltagged CH_4 masses exactly match the mass calculated inof the reference simulationtracer with all sources, which confirms the linearity of the system with chemical feedbacks suppressed through the fixed oxidant

distributions. Seasonal global mass variations in individual contributions from constant sources are caused by OH-chemistry and dynamics, e.g. by the migrating ITCZ.

4.1.1 NOAA/AGAGE~~/NOAA~~ stations

Based on the a priori emission assumptions (~~Tab.~~Table 1, col. ~~2~~3) the ~~1997 – 2000~~ through 2006 average CH_4 mixing-ratio over all AGAGE/NOAA stations of ~~1789~~1,780 nmol/mol is simulated within a Root Mean Square deviation (RMS) of 0.~~51~~40 %. With the applied initial distribution ~~(scaled to match the observations)~~ and emissions, the model reproduces both the 1997-1999 trend and the period without trend from 2000-2006. This suggests that the global CH_4 concentration in the period 2000-2006 represents the steady state after previously increasing emissions, probably until the early 1990s.

~~Consistently~~Consistent with the observations, the simulated CH_4 mixing ratios are largest at ~~MHD (53~~BRW (71°N) and decrease with latitude, reaching ~~a~~ minimum values south of 40 °S at CRZ (46°S), HBA (76°S), and SPO (90°S). The abundance at AGAGE CGO (41°S~~),~~) is slightly enhanced and scattered, being exposed to pollution events from the Australian continent, but also well reproduced by the model. The 2000-2006 (no-trend period) average observed mean mixing ratios for these stations range from ~~1864~~1,865 to ~~1734~~1,727 nmol/mol and ~~could be reproduced~~, using a-priori emissions, are simulated within an average percentage RMS ~~of~~= 0.~~88 % and 0.37 % respectively,~~67 %. Northern Hemispheric values however~~, being too high~~ are overestimated, e.g. at BRW by ~~12~~18.2 nmol/mol (0.98 %) much more than the 5.7 nmol/mol (0.~~64 %) at MHD and too low by 5 nmol/mol (0.29~~33 %) at ~~CGO, indicating a possible mismatch in the emission assumptions, which is reflected in~~SPO (North Pole) and cause an excessive interhemispheric ~~CH_4 gradient ΔNS. If we define ΔNS as the~~ difference ~~between average CH4 mixing ratios at the northern stations MHD (53°N) and THD (41ºN) and the southern station CGO (41ºS) for the years 2000 – 2006, the model ΔNS of 135 nmol/mol appears too large compared to the observed 118 nmol/mol~~(Fig. 3, red/yellow dotted vs blue) indicating mismatches in the emission assumptions. Although this imparity could also be caused by erroneous interhemispheric transport, previous analyses (Aghedo et al.2010, Krol et al. 2017) show that the underlying ECHAM5 model reproduce realistically the Inter-hemispheric transport time.

Taking advantage of the Solver (Sect. 2.2) we defined the goal as the minimum RMS deviation between the station measurements and respective model simulations composed of the tagged components multiplied with scaling factors, i.e. the parameters. Likely tolerance intervals (constrains) are available in form of uncertainty specifications along with the a-priori emission assumptions (e.g. Bergamaschi et al., 2013). The largest interval (12%) is allowed for the category gas production.

The a-priori simulation results (Fig. 3, black crosses), as mentioned above, are too high in the Northern Hemisphere compared to the observations (blue) suggesting overestimated emission assumptions there. The Solver consequently calculates a 20.6 Tg CH_4 /y reduction of fossil fuel emissions (predominantly coal and gas) in favor of an 18.8 Tg/y increment in the other sources (predominantly tropical wetlands, rice paddies, and biomass burning) to fit the observations (Fig. 3, red solid line). The optimization effect on the emission categories is summarized in Table1, col. 4 and graphically displayed in Fig. S4 (supplement). Hence, the net reduction of just 1.84 Tg/y (0.32 % of the total) underlines the general consistency of the a-priori assumptions, while the necessity of the redistribution among the uncertain emissions by source category (Dlugokencky et al. 2011). The RMS deviation from the all-station average mole fraction improves to 7.17 (0.40 % of the all-station 2000-2005 mean). The all station coefficient of determination $R^2 = 0.80$ confirms the good agreement with observed variability (see scatter plots in Fig. 4 for individual stations ALT,

RPB, and SPO). The calculated 2000-2006 average interhemispheric methane difference between extreme NH and SH stations of 131 nmol/mol improves by a factor of 12 and matches the observations up to 0.76 %. Fig. ~~The tagging approach offers a way to rescale emission amounts of individual sources with proportional effects on the global distribution. An emission increment in the tropical wetland source (SWA) along with a reduction of nearly the same amount of the fossil group of categories comprising landfill , coal , gas , and oil (FOS) appears to be appropriate to improve the latitudinal CH_4 distribution. The model to observation RMS deviation as a function of a FOS to SWA redistribution amount follows a 2nd order polynomial shape with minimum RMS = 0.37 % at 24.7 Tg/y (Fig. 4a – blue line). The corresponding ΔNS dependency follows a linear function with root at 30.6 Tg/y (Fig. 4a – red line). The range between the optima in RMS and ΔNS is a consequence of the relatively course discrimination of the contributing sources into SWA and just FOS. The average redistribution value of 28.7 Tg/y in form of a RMS/ΔNS combined optimum is applied in the following (Table 1, col. 3), especially as a basis for the 2007 – 2014 methane trend simulation. The average mixing ratios at the stations in latitudinal order are plotted in Fig. 4b.~~

~~In Fig. 5 the observed CH_4 records at our reference stations 1997 – 2006 are plotted in blue together with the standard deviations and compared to model results (red) gained with the a posteriori emissions. The seasonality, with a maximum in NH winter, is apparent at MHD, but is more pronounced and less scattered at THD, RPB and MLO. Near the Equator (e.g. SMO, 14° S) the seasonal cycle is weakest, while at CGO in the SH we find a phase shift by six months compared to NH stations. Regression analysis (Fig. 6) shows that the coefficient of determination is highest at CGO (R^2 = 0.92) but still highly significant at MHD (0.84), despite that the station is relatively close to methane sources and relatively frequently affected by synoptic scale pollution events from the European continent. Please refer to Table 2, row C4 for R^2 and row C3 for the RMS at all stations.~~

~~At MLO (3397masl) the offset of -287 nmol/mol together with the slope of 1.16x indicates an underestimation of low CH_4 values there and can be attributed to increasing vertical model grid resolution with altitude; i.e. the amplitude is reduced but the average preserved.~~

~~The tagged tracer simulations~~ 5 shows the final simulation results based on the revised emissions together with the measurement at five representative observation sites. The initial distribution, which is the result of a long term simulation, does not precisely reflect the special Jan. 1997 situation, but obviously overestimated starting values at northern hemispheric stations level out in the course of the first year. The Solver cannot improve this because it acts on the whole 4d tracer distribution time series and not on individual years.

The tagged tracers indicate that the atmospheric ~~concentrations during~~mixing-ratios over the ~~stable phase~~years 1997 through 2006 are proportional to the respective emission amounts, but influenced by the distance from the source due to the oxidation by OH. Footprints at stations are the result of source and sink interaction (Fig. ~~7). Emissions that take place relatively close to the main sinks (i.e. predominantly tropical OH) have~~S5). A shorter distance leads to a reduced atmospheric abundance relative to the source strength and vice versa. ~~Particularly boreal biomass burning emissions with accumulating concentrations over the NH (Fig. S3a) have an extended lifetime of 8.92 years, compared with rice paddy emissions, which are subject to injection into the tropical global OH maximum (~~This is quantified in terms of "steady state lifetime", defined as the ratio between the global atmospheric trace mass (i.e. atmospheric burden) and the annual emission amount, which is , by definition of steady state, equal the total annual sink. Over the period of relative stagnation 2000 – 2006 (Fig. 1) the shortest lifetimes ($\tau \cong 7.3$ years) were found for fossil methane being emitted predominantly by industrialized countries, from landfills and oil production in the Northern Hemisphere and therefore experiencing the highest OH concentrations (Fig. 6). On the other hand, wetland methane is exposed to lower OH concentration, producing a steady state lifetime of τ = 10.08 years (Table 1, col. 5 and Fig. S6). Biomass burning

methane never establishes steady state equilibrium because of the very irregular inter-annual intensity of the fire events. Considering that its contribution to the total~~Fig. S3b) and relatively short lived (8.34 y). All stations are more than 25 % exposed to tropical and southern hemispheric swamp released methane, ranging from 25.8 % at MHD, 53°N to 28.9 % at CGO, 40°S. Landfill~~ emissions~~, for example, are less intense than those of swamps and predominantly released in the NH. Their footprint at stations undergoes an opposite (north/south) gradient (Fig. 8).~~ with ~3.5 % is small, the quantification of the total CH_4-lifetime $\tau \cong 8.45$ years appears reasonable.

From 2007 on, when the station records show an upward trend (cf. Fig. 1 representatively for ~~CGO~~SPO) additional emissions ~~are~~were necessary in order to close the budget if the sink processes are kept unchanged. The simulation for this period is presented in ~~Ch~~Sect. 4.2.

4.1.2 CARIBIC flights

The spatio-temporal distribution of the CARIBIC CH_4 sampling is quite different from that of the surface stations. Measurements ~~are~~were taken over relatively short time intervals and more than 96 % of the samples are from the NH. In contrast to the monthly average station data, the CARIBIC individual methane observations in the ~~Upper Troposphere and Lower Stratosphere (UTLS)~~UTLS are based on air sampling over 20 minutes (i.e. ~300 km) for CARIBIC-1 and about two minutes (i.e. ~30 km) for CARIBIC-2 and compared to the stations appear to be much more variable. The sequence of sampling is irregular in time, i.e. the same destinations are reached through different flight routes (Fig. ~~S2~~2b), and take place ~~at~~during different times of the year. Thus the following statistics are not comparable to the station observations.

Between 2000 and 2006, ~~the average of~~ all ~~simulated methane samples based on the a posteriori emission data is 1781 nmol/mol while the corresponding~~ CARIBIC observations average at ~~1786~~1,786 nmol/mol. Corrected with respect to the a-posteriori emission data based on the station analysis, the simulation average comes as close as 1,788 nmol/mol ~~with a~~. The whole period is fairly well reproduced within an RMS deviation of 1.~~05~~01 % and a coefficient of determination $R^2 = 0.65$ (Table 3, rows C1-4). The scattered sampling positions cannot be accurately reproduced by the grid model EMAC, because of its limited resolution. The observed CH_4 variability features short-duration events like the interception of methane plumes or alternatively relatively clean air episodes and ~~even~~especially stratospheric air, however, the patterns are rather well reproduced (Fig. ~~9~~7). The model appears to capture the variations well, even those which are subject to intercepting upper tropospheric and lowermost stratosphere at mid and higher latitudes.

The amplitudes of the model time series, however, are smaller due to the relatively coarse vertical grid spacing of the model, which represents the UTLS at a vertical resolution of about 500m – compared to ~45m near surface. In contrast to background station measurements, for the CARIBIC time series local maxima and minima are not only related to season but also to vertical gradient effects, especially due to the strong concentration changes across the tropopause. The scatter plot (Fig. ~~10~~8, upper left) shows a regression slope of 0.~~54~~57, i.e. well below 1, which quantifies the evident underestimation of the calculated CH_4 variability in the graphs of Fig. ~~9~~7, suggesting that the vertical resolution of the model grid is not optimal to resolve the fine structure in the tropopause region. The slope is compensated by a corresponding offset~~,~~ up to ~~817~~766 nmol/mol, explaining the good ~~agreement~~congruence between simulations and observations in Fig. ~~9~~7.

For further analysis, according to the definition in Sect. 3.2 (Fig. ~~S3),~~ 2b), we grouped the data records in Fig. ~~S4~~S7 by the 7 flight sampling regions: EUR, AFR, FAE, IND, NAM, SAN, and SAS. The best agreement between model and observations in terms of RMS is achieved over low-latitude regions such as IND with 0.~~75~~80 % and SAN/SAS $\leq$ 0.~~87~~

%, while75. Here the effect of stratospheric air is least. At the same time, observations over continental areas in the mid latitude NH still could be simulated within a RMS range of 1.2023 % (EUR) and 1.3424 % (FAE). It appears that the variance of the CARIBIC measurements is with R^2 > 0.60 is fairly well reproduced everywhere and most accurately reproduced over EUR with R^2 = 0.74 and over IND with R^2 = 0.65.82 (Fig. 8). AFR is not discussed here because of the sparse number of samples of 5.9 %.4.7 % of all. The statistics are summarized in (Table 32, rows C1-5).

4.2 Simulating the recent methane trend

In accordance with The measured methane increase, depicted by the CGOblue lines in Fig. 9a for the NOAA background station data (SPO (90°S) and in Fig. 11a, blue line),9b for the CARIBIC measurements show a significant methane increase from 2007 onward (Fig. 11b, blue line), which flight records, cannot be reproduced by the model (red) cannot reproduce under the assumption of lines) based on inter-annually constant emissions. This Between 2007 and 2013 the slope appears nearly linear (Fig. 1), and the discrepancy iscan be removed by assuming an additional inter-annually constant CH_4 source starting in 2007. for this period. We find that after 2013 an additional increment is necessary to fit the trend.

Encouraged by our tagging results, an EMAC model sensitivity study was set up with additionalenhanced emissions from the tropical wetlands (scenario TRO) and an additional source from North American shale gas (scenario SHA) drilling sites, to resolve the post-2006 model – observation discrepancy mentioned above.. Enhanced precipitation in the regional summer season (Nisbet et al., 20142016; Bergamaschi et al., 2013) may be a possible cause of higher growing tropical wetland emissions. To create a "fracking" map we relied on the publicly available database maintained by the national hydraulic fracturing chemical registry (FracFocus, 2016). Fig. Figs. 12aS2a and b show the global CH_4 mixing ratios near the surface, logarithmically scaled for better visibility, marking the respective hypothetical emissions. While the assumed Amazontropical and N North American emission fluxes aremay be identical, the former are more efficiently mixed vertically due to deep tropical convection (Figs. S5aFig. S3a, b) and therefore lead to smaller enhancements near the surface.

For the amount of additional emissions, we used the upper estimate from Bergamaschi et al. (2013) of 22 Tg CH_4/yr as a first guess of emissions to be added in order to fit the upward trend. The resulting slope of CH_4 increase over the years 2007 to 2014 at the station CGO turned out to be underestimated by a factor of 1.3, motivating a further increase in emissions. This increase of the emission also closes the budget during the previous no methane trend years, pointing out that a decreasing of OH during the trend period is unlikely. Optimal agreement at CGO was achieved by adding a total of 28.3 Tg/y and was used as input for tagged simulations of scenarios TRO and SHA. Both scenarios perfectly reproduce the observed CH_4 trend, but affect the RMS deviation at NH, SH, and tropical stations in different ways. To further optimize the agreement between model and measurements combinations of both scenarios have been evaluated.

We used an upper limit emission of 28 Tg/CH_4/y to be added in order to fit the upward trend between 2007 and 2013. Separate tagged simulations of TRO and SHA were performed with this source starting in Jan. 2007. The Solver was applied to optimize the combination of fractional amounts of TRO and SHA to be added to the non-trend results after 2006 with the constraint to fit the seventeen station records with minimum RMS deviation.

Note that in this work we focus on the sourcessource strengths and neglect inter-annual changes in global OH, which are assumed to be small (Nisbet et al., 2016). Changes in the removal rate of methane by the OH radical have not been seen in other tracers of atmospheric chemistry, e.g. methyl chloroform (CH_3CCl_3) (Montzka et al., 2011; Lelieveld et al. 2016; Schaefer et al., 2016).) and do not appear to explain short-term variations in methane. Based on numerical

analyses Turner et al. (2017) found that a combination of decreasing methane emissions overlaid by a simultaneous reduction in OH concentration (the primary sink) could have caused the renewed growth in atmospheric methane. However, they could not exclude rising methane emissions under time invariant OH concentrations as a consistent solution to fit the (rising) observations. Changes of the order of 3-5% per year over an 8 year period appear very unlikely.

In the next sections, more detailed analyses are presented to evaluate the two scenarios. ~~Changes in the order of 3-5% per year over a 8 year period are very unlikely.~~

4.2.1 NOAA and AGAGE/~~NOAA~~ stations

~~Shale gas associated~~Methane emissions~~, originating mostly~~ from ~~the northern hemisphere, need a relatively longer time to influence CH_4 at southern hemispheric stations like Cape Grim, Tasmania (CGO), compared with to those from the~~ tropical wetlands~~. The latter appear to also~~ affect northern as well as Southern Hemispheric observations ~~e.g. at Mace Head, Ireland (MHD).~~approximately similarly. Under the influence of deep convection in the tropics and subsequent global transport, the characteristic seasonality of tropical wetland emissions can significantly influence the CH_4 time series worldwide. Shale gas associated emissions from the Northern Hemisphere need a relatively longer time period to influence CH_4 at southern hemispheric stations like South Pole (SPO, 90° S). We use the model results together with the measurement data to estimate to which extend ~~presumed~~possible increases in these tropical and extratropical CH_4 sources can provide a plausible explanation for the observed recent trend.

~~As mentioned before,~~ After introducing ~~an emission increment~~ the additional emissions of 28~~.3 Tg~~CH_4 Tg CH_4/y ~~starting in~~from 2007 ~~for matching the global growth of CH_4~~on, the ~~observed trend is reproduced well~~CH_4 increments are calculated at all ground stations in both scenarios (TRO and SHA~~. Similarly to~~). At first glance an overall offset indicates an overestimation for both scenarios. Applying the TRO scenario exclusively leads to an all-station RMS = 7.1 % of the respective total abundance. The SHA scenario approaches the all-station mean within RMS = 10.4 %. The deviation from the interhemispheric CH_4 difference ΔNH/SH in both cases with 143 and 127 nmol/mol is much too high compared to the observed 133.84. A suitably downgraded best fitting combination of TRO and SHA, in the same way as for the no-trend period ~~(see~~, can be found by the applying the Solver:

For the years 2007 through 2013 it turns out that a total emission of 20.70 Tg CH_4/y composed of 12.33 Tg TRO and 8.38 Tg SHA reduces the RMS to 0.55 %, and approximates the observed ΔNH/SH = 133.84 up to 99.5 % (modelled difference is 133.14). Fig. ~~4a), the relative contribution of TRO and SHA has been obtained by minimizing the ΔNS and RMS with respect to the~~ 10 shows the CH_4 observations (~~Fig. 13a, solid lines). The~~ blue) at all stations considered from North to South together with the respective no-trend simulations (black crosses) and the Solver-optimized ~~contribution is 62.7 % (17.7 Tg/y) for TRO and 37.3 % (10.6 Tg/y)~~TRO / SHA increment which approaches the observations within least RMS (red dots). High latitude mixing ratios (north and south) are slightly overestimated by 0.25 % in average.

The scatter plots for ~~SHA.~~ the trend period through 2013 (Fig. 11) indicate good correlation between the observed and calculated station monthly means. Selected NOAA stations records are displayed in Fig. 12, continuing the 1997 through 2006 course (Fig. 8) with added scaled TRO- and SHA emissions.

With respect to longitudinal dependency of the SHA emissions, two control simulations were initiated, one with additional emissions from East Asia (FAE: 25° N – 50° N, 100° E - 150° E) and another with additional emissions from Europe (EUR: 45°N – 60°N, 0° - 26°E). ~~The optimization procedure (see Fig.13a, dashed and dotted line for FAE and EUR simulations, respectively) reveals different source fractions for the minima of ΔNS and RMS (see Fig.13a, colored symbols and arrows). This shows that, when the SHA emissions are located away from the North America, no fraction~~

is found that could minimize simultaneously the ΔNS and RMS. On other hand, the discrepancy between the minima of ΔNS and RMS for the scenario with SHA emissions over North America (marked by yellow collate symbols) is very small (within 1%), indicating a realistic latitudinal positioning of the source region. While no significant trend impact could be assigned to EUR, by just numerical optimization a hypothetical FAE contribution cannot be excluded. No evidence in favor of SHA or FAE can be detected at one of the stations in the northern hemispheric mid-latitudes presumably due to relatively intense latitudinal mixing and the >8 year lifetime of CH_4. Kirschke et al. (2013) and Turner et al. (2016), however, found that an increase by 17-22 Tg/y could explain the renewed methane growth and 30-60% of this could be attributed to increasing U.S. anthropogenic methane emissions, which supports our results with 20.70 Tg/y emission increase including 8.38 Tg/y (40 %) SHA.

The scatter plots for the North American reference SHA (Fig. 14) indicate fairly good correlation between the observed vs. calculated station monthly means for the period after 2007. Statistics for the trend simulations are given in Table 2, rows T1-5, including the averaged observed and calculated mixing ratios, their deviation in terms of RMS (%) and the coefficient of determination R^2. All trend simulation results at AGAGE/NOAA stations are summarized in Fig. 15.

4.2.2 CARIBIC flights

Based on the same optimized emission scenario (62.6 %12.33 Tg CH_4/y TRO/ 37.4 % and 8.38 SHA) the trend in the post-2006 CARIBIC-2 methane measurements appears to be realistically simulated by the EMAC model as well. In Fig. 1613 monthly averaged CARIBIC measurements are plotted together with corresponding model results. The slopes of the linear trend lines 0.32x (CARIBIC) and 0.31x (EMAC) over time inwhere x = number of months over the 8 flight observation years 2007 through 2014, indicating (the latest record considered in this study), indicate a very good model representation of the methane trend. The regression analysis with R^2 = 0.8 over all flight samples (Fig. S714, upper left panel) over all flight samples even improves for this period, possiblyprobably also due to a much higher sampling density. As mentioned before, the model underestimates the measured extremes, especially negative peaksdownward excursions observed during northern hemispheric intercontinental flights in April and May 2009, '112011, and '122012 caused by tropopause folds, which at the given vertical grid spacing (~500 m in the respective altitude regionUTLS) cannot satisfactorily be resolved by the model. This is confirmed by the frequency spectrumsspectra (Fig.17) confirm this: 14): median simulated values reveal higher amplitudes than measurements before and during the methane-trend period. The different widths of the frequency distributions σ = 6.2 (EMAC) and 4.7 nmol/mol (CARIBIC) for the period 2007-2014 and σ = 7.4 and 6.3 nmol/mol, respectively, for the period 2000-2006 confirms the model biasingfavoring medium range values.

For detailed comparison with the pre-2007 results Fig S6a. 16 depicts the whole series unresolved however on a non-equidistant time axis. Focusing on individual flight sampling regions (Fig S6b. S8) we restrict the statistical analyses to those areas having and periods with at least 300 samples. The highest coefficients of determination (R^2 >0.8) are obtained for NANNAM, EUR and the FAE. For the other four regions reaching further south such as SAN or IND, the tropopause influence of the lower stratosphere is stronger, leading to reduced linear slopes together with comparably less R^2 of 0.5859 and 0.72 (cf. Fig. S7 for diagrams14).

4.2.2.1 Selected CARIBIC flights

Individual flights show variations in CH_4 source composition in response to relatively small scale influences. A striking demonstration of the varying influences of emissions in the model in regions crossed by the CARIBIC aircraft is

provided by flights 244-245 on August 13–14, 2008, between Frankfurt in Germany and Chennai (formerly Madras) in India. In Fig. ~~18a~~17a (right ordinate) the total observed CH_4 mixing ratios along the flight track are plotted over the respective simulations (with and without TRO/SHA-trend increment~~. Like at all flights~~). Typically, simulated peak values ~~for this flight~~ are underestimated and not correctly in phase with the observations. Fig. ~~18b~~17b underlines this for the whole collection of India bound CARIBIC flight samples in accordance with Fig~~17~~. 15. The TRO/SHA increment in Fig. ~~18a~~17a is obvious but with 0.8 % on average still relatively small in 2008. The source segregated rice paddy-methane (green, left ordinate) dominates the pattern of the total CH_4 and the R^2 = 0.~~58~~65 implies that 0.~~58~~65 % of the observed CH_4 variability along this special flight track can be explained by rice paddy emissions. ~~Highest~~Largest mixing ratios in excess of ~~1850~~1,850 nmol/mol were recorded in the upper troposphere between 50° and 75° E. Trajectory calculations as well as methane isotope and other chemical tracer analyses (Schuck et al~~.~~., 2012~~;~~; Baker et al~~.~~., 2012) corroborate that these air masses carry emissions from South and Southeast Asia and can be explained by the trapping of air masses (Rauthe-Schöch et al~~.~~., 2016) from South Asia in the Upper Troposphere Anticyclone (UTAC), a persistent phenomenon during the monsoon and centered over Pakistan and northern India (Garny and Randel, 2013). This is also qualitatively illustrated in Fig. ~~19b.~~S9a,b. The ~~upper tropospheric~~methane released by rice paddies in South Asia, trapped ~~regional rice paddy released methane~~ in the UTAC, obviously marks the local maximum in the total CH_4 distribution (Fig. ~~19a~~S9b - different scales were used for better representation). The flight route crosses this pattern twice, from NW to SE and back. Further, relatively localized maxima in the northern hemispheric extra-tropics (red areas in Fig. ~~19a~~S9a) are caused by anthropogenic sources such as coal mining and gas exploitation and from the high latitude bogs in summer.

Another demonstrative example for tagging results is presented in Fig. ~~20~~S10 which depicts CH_4 mixing-ratios observed during the Far East flight 304 from Osaka, Japan to Frankfurt (Main), Germany in July 2010 together with respective ~~simulations~~tracers including four of the most relevant individual tagged source contributions. Calculations (red dashed, right axis) follow the phase of the measurements (blue dashed, right axis). The trend period increment (the difference between red fat and red thin lines) in 2010 with 1.~~44~~22 % in average has almost doubled compared to 2008. The pattern is ~~obviously~~ determined by animal-, landfill-, and natural gas source contributions. The determination coefficients with respect to the observations ~~amount~~amounts to R^2 = 0.~~83, 0.78, and 0.66 respectively.~~77. The pronounced bog-methane profile (color coded in olive-green) dominates the pattern but is not correctly in phase with CARIBIC in terms of an R^2 = 0.38. Rice fields east of 136°E contribute ~~above average~~relatively strongly.

~~The~~A more systematic study of the source segregated composition of all 327 CARIBIC flights over the years 1997 through 2014 with special emphasis on the developing trend beyond ~~is~~will be subject of ~~a separate~~continued investigation.

5 Conclusion and Outlook

We analyzed the atmospheric methane budget by means of ~~the~~ EMAC model simulations and comparing ~~simulations~~the results with data from ~~selected~~NOAA and AGAGE~~/NOAA~~ surface stations and CARIBIC aircraft data. Source tagging is used to analyze the emission distribution and to optimize the model results with respect to the observations. We found that, compared to our a-priory assumptions, a larger ~~Amazon wetland~~natural methane source with a concomitant reduction in NH fossil emissions is required to explain the measurements and especially the observed interhemispheric gradient.

Two possible additional methane sources, shale gas extraction (SHA) and tropical wetlands (TRO) have been investigated, that could cause the resuming methane growth since 2007. We showed that a methane increase of ~~28.3~~20.70 Tg/y in 2007 and subsequent years, of which ~~60 %~~12.33 from TRO and ~~40 %~~8.38 from SHA, can optimally explain the recent CH_4 trend until 2013.

In view of the additional global CH_4 source since 2007, a source – sink equilibrium has not yet been established after the 8 years of emissions considered. A 2nd order polynomial extrapolation predicts steady state after 13 years ~~supposed~~, assuming that the emissions remain unchanged~~.~~, which does not seem realistic in view of the observed development after 2013/14 (Fig. 1). We are aware that there is no unique solution for the source – receptor relationship. Therefore, the emissions used in this work must be considered as more representative of latitudinal emissions~~, not representing the real location~~ than of ~~the~~ emissions from specific locations. Nevertheless, the degree of freedom in the choice of sources is limited and our scenario realistically represents the north-south gradient of CH_4, a critical constraint ~~as corroborated by the "Far East" and "Europe" control simulations.~~.

NOAA/AGAGE~~/NOAA~~ station methane data are ~~currently available through September 2015 and~~updated annually so further updates are expected. CARIBIC flight measurements ~~are analyzed and data are available through February 2016.~~have been resumed (after a one-year break). We plan to continue the study of these data, supported with EMAC model simulations, also taking advantage of the ~~resuming~~most recent and future CARIBIC flights ~~in 2017/18~~. A larger coverage of Southern Hemispheric sampling routes would ~~desirably~~be desirable to extend the database ~~for explaining~~and help explain the ongoing, and possibly accelerating upward methane trend.

Acknowledgements:

CARIBIC relevant activities of this modeling project were carried out under contract 320/20585908/IMK-ASF-TOP/GFB by Karlsruhe Institute of Technology (KIT), Karlsruhe.

AGAGE is supported principally by NASA (USA) grants to MIT and SIO, and also by: DECC (UK) and NOAA (USA) grants to Bristol University; CSIRO and BoM (Australia): FOEN grants to Empa (Switzerland); NILU (Norway); SNU (Korea); CMA (China); NIES (Japan); and Urbino University (Italy)

References

Aalst van, M. K., van den Broek, M. M. P., Bregman, A., Brühl, C., Steil, B., Toon, G. C., Garcelon, S., Hansford, G. M., Jones, R. L., Gardiner, T. D., Roelofs, G.-J., Lelieveld, J., and Crutzen, P. J.: Trace gas transport in the 1999/2000 Arctic; comparison of nudged GCM runs with observations, Atmos. Chem. Phys., 4, 81-93, 2004, http://www.atmos-chem-phys.net/4/81/2004/.

Aardenne van J. A. et al.: The EDGAR 3.2 Fast Track 2000 dataset (32FT2000), http://themasites.pbl.nl/tridion/en/themasites/edgar/emission_data/edgar_32ft2000/documentation/index-2.html

Aardenne van J. A., F. J. Dentener, J. G. J. Olivier, J. A. H. W. Peters, and L. N. Ganzeveld (2005), The EDGAR 3.2 fast track 2000 dataset (32FT2000), technical report, Joint Res. Cent., Ispra, Italy. (Available at http://themasites.pbl.nl/tridion/en/themasites/edgar/emission_data/edgar_32ft2000/documentation/index-2.html.)

Baker A., T. J. Schuck, C. A. M. Brenninkmeijer, and Armin Rauthe-Schöch, Estimating the contribution of monsoon-related biogenic production to methane emissions from South Asia using CARIBIC observations, Geophys. Res. Lett., 39, L10813, doi:10.1029/2012GL051756, 2012.

Bergamaschi P., S. Houweling, A. Segers, M. Krol, C. Frankenberg, R. A. Scheepmaker, E. Dlugokencky, S. C. Wofsy, E. A. Kort, C. Sweeney, T. Schuck, C. Brenninkmeijer, H. Chen, V. Beck, and C. Gerbig (2013), AtmosphericCH4 in the first decade of the 21st century: Inverse modeling analysis using SCIAMACHY satellite retrievals and NOAA surface measurements, J. Geophys. Res. Atmos., 118, 7350–7369, doi:10.1002/ jgrd.50480.

Brenninkmeijer C. A. M., Crutzen, P., Boumard, F., Dauer, T., Dix, B., Ebinghaus, R., Filippi, D., Fischer, H., Franke, H., Fries, U., Heintzenberg, J., Helleis, F., Hermann, M., Kock, H. H., Koeppel, C., Lelieveld, J., Leuenberger, M., Martinsson, B. G., Miemczyk, S., Moret, H. P., Nguyen, H. N., Nyfeler, P., Oram, D., O'Sullivan, D., Penkett, S., Platt, U., Pupek, M., Ramonet, M., Randa, B., Reichelt, M., Rhee, T. S., Rohwer, J., Rosenfeld, K., Scharffe, D., Schlager, H., Schumann, U., Slemr, F., Sprung, D., Stock, P., Thaler, R., Valentino, F., van Velthoven, P., Waibel, A., Wandel, A., Waschitschek, K., Wiedensohler, A., Xueref-Remy, I., Zahn, A., Zech, U., and Ziereis, H.: Civil Aircraft for the regular investigation of the atmosphere based on an instrumented container: The new CARIBIC system, Atmos. Chem. Phys., 7, 4953-4976, doi:10.5194/acp-7-4953-2007, 2007.

Brenninkmeijer C.A.M. , P. J. Crutzen , H. Fischer , H. Güsten , W. Hans , G. Heinrich , J. Heintzenberg , M. Hermann , T. Immelmann , D. Kersting , M. Maiss , M. Nolle , A. Pitscheider , H. Pohlkamp , D. Scharffe , K. Specht , and A. Wiedensohler , 2010: CARIBIC-Civil Aircraft for Global Measurement of Trace Gases and Aerosols in the Tropopause Region. Journal of Atmospheric and Oceanic Technology, 16, 1373-1383, doi: 10.1175/1520-0426(1999)016<1373:CCAFGM>2.0.CO;2.

Brenninkmeijer C.A.M. , P. J. Crutzen, F. Boumard, T. Dauer, B. Dix, R. Ebinghaus, D. Filippi, H. Fischer, H. Franke, U. Frieß, J. Heintzenberg, F. Helleis, M. Hermann, H. H. Kock, C. Koeppel, J. Lelieveld, M. Leuenberger, B. G. Martinsson, S. Miemczyk, H. P. Moret, H. N. Nguyen, P. Nyfeler, D. Oram, D. O'Sullivan, S. Penkett, U. Platt, M. Pupek, M. Ramonet, B. Randa, M. Reichelt, T. S. Rhee, J. Rohwer, K. Rosenfeld, D. Scharffe, H. Schlager, U. Schumann, F. Šlemr, D. Sprung, P. Stock, R. Thaler, F. Valentino, P. van Velthoven, A. Waibel, A. Wandel, K. Waschitschek, A. Wiedensohler, I. Xueref-Remy, A. Zahn, U. Zech, and H. Ziereis, Civil Aircraft for the Regular Investigation of the atmosphere Based on an Instrumented Container: The new CARIBIC system. Atmospheric Chemistry and Physics (ACP) 2007

Ciais, P., C. Sabine, G. Bala, L. Bopp, V. Brovkin, J. Canadell, A. Chhabra, R. DeFries, J. Galloway, M. Heimann, C. Jones, C. Le Quéré, R.B. Myneni, S. Piao and P. Thornton, 2013: Carbon and Other Biogeochemical Cycles. In: Climate Change 2013: The Physical Science Basis. Contribution of Working Group I to the Fifth Assessment Report of the Intergovernmental Panel on Climate Change [Stocker, T.F., D. Qin, G.-K. Plattner, M. Tignor, S.K. Allen, J. Boschung, A. Nauels, Y. Xia, V. Bex and P.M. Midgley (eds.)]. Cambridge University Press, Cambridge, United Kingdom and New York, NY, USA.

Crutzen P. J.: The " anthropocene ", J. Phys. IV France 12 (2002), DOI : 10. 1051/j:p2 40 020447

Cunnold D.M., L.P. Steele, P.J. Fraser, P.G. Simmonds, R.G. Prinn, R.F. Weiss, L.W. Porter, R.L. Langenfelds, H.J. Wang, L. Emmons, X.X. Tie, and E.J. Dlugokencky, In situ measurements of atmospheric methane at GAGE/AGAGE sites during 1985-2000 and resulting source inferences. J. Geophys. Res., 107, D14, doi: 10.1029/2001JD001226, 2002.

Curry C. L. (2007), Modeling the soil consumption of atmospheric methane at the global scale, Global Biogeochem. Cycles, 21, GB4012, doi:10.1029/2006GB002818.

Dee, D. P., Uppala, S. M., Simmons, A. J., Berrisford, P., Poli, P., Kobayashi, S., Andrae, U., Balmaseda, M. A., Balsamo, G., Bauer, P., Bechtold, P., Beljaars, A. C. M., van de Berg, L., Bid-lot, J., Bormann, N., Delsol, C., Dragani, R., Fuentes, M., Geer, A. J., Haimberger, L., Healy, S. B., Hersbach, H., Hólm, E. V., Isaksen, L., Kållberg, P., Köhler, M., Matricardi, M., McNally, A. P., Monge-Sanz, B. M., Morcrette, J.-J., Park, B.-K., Peubey, C., de Rosnay, P., Tavolato, C., Thépaut, J.-N., and Vitart, F.: The ERA-Interim reanalysis: configuration and performance of the data assimilation system, Q. J. Roy. Meteor. Soc., 137, 553–597, doi:10.1002/qj.828, 2011.

Dentener F., Kinne, S., Bond, T., Boucher, O., Cofala, J., Generoso, S., Ginoux, P., Gong, S., Hoelzemann, J. J., Ito, A., Marelli, L., Penner, J. E., Putaud, J.-P., Textor, C., Schulz, M., van der Werf, G. R., and Wilson, J.: Emissions of primary aerosol and precursor gases in the years 2000 and 1750 prescribed data-sets for AeroCom, Atmos. Chem. Phys., 6, 4321-4344, doi:10.5194/acp-6-4321-2006, 2006.

Dlugokencky E., E. J., R. C. Myers, P. M. Lang, K. A. Masarie, A. M. Crotwell, K. W. Thoning, B. D. Hall, J. W. Elkins, and L. P. Steele (2005), Conversion of NOAA atmospheric dry air CH4 mole fractions to a gravimetrically prepared standard scale, J. Geophys. Res., 110, D18306, doi:10.1029/2005JD006035. J., E. G. Nisbet, R. Fisher, D. Lowry, Global atmospheric methane: budget, changes and dangers Philos. Trans. R. Soc. London Ser. A 369, 2058 (2011).

Dlugokencky, E. J., L. Bruhwiler, J. W. C. White, L. K. Emmons, P. C. Novelli, S. A. Montzka, K. A. Masarie, P. M. Lang, A. M. Crotwell, J. B. Miller, and L. V. Gatti, Observational constraints on recent increases in the atmospheric CH4 burden, Geophys. Res. Lett., 36(L18803), doi: 10.1029/2009GL039780, 2009.

Dlugokencky, E. J., E. G. Nisbet, R. Fisher, and D. Lowry, Global atmospheric methane: budget, changes and dangers, Phil. Trans. R. Soc. A 369(1943), 2058-2072, doi: 10.1098/rsta.2010.0341, 2011.

Dlugokencky, E.J., P.M. Lang, A.M. Crotwell, J.W. Mund (2016), , M.J. Crotwell, and K.W. Thoning (2018), Atmospheric Methane Dry Air Mole Fractions from quasi-continuous measurements at Barrow, Alaska and Mauna Loa, Hawaii, 1986-2015the NOAA ESRL Carbon Cycle Cooperative Global Air Sampling Network, 1983-2017, Version: 20162018-08-01 22, Path: ftp://aftp.cmdl.noaa.gov/data/trace_gases/ch4/in-situflask/surface//.

Etminan, M., G. Myhre, E. J. Highwood, and K. P. Shine (2016), Radiative forcing of carbon dioxide, methane, and nitrous oxide: A significant revision of the methane radiative forcing, Geophys. Res. Lett., 43, 12,614 – 12,623, doi:10.1002/2016GL071930.

Frank, F. I.: Atmospheric methane and its isotopic composition in a changing climate, Ph.D. thesis, Ludwig-Maximilians-Universität, München, URL http://nbn-resolving.de/urn:nbn:de:bvb:19-225789 (2018)

FAO, 2010: http://foris.fao.org/static/data/fra2010/StateofForests_Report_English.pdf

Forster P. et al. 2007 Changes in atmospheric constituents and in radiative forcing. In Climate change 2007: the physical science basis. Contribution of Working Group I to the Fourth Assessment Report of the Intergovernmental Panel on Climate Change (eds S. Solomon, D. Qin, M. Manning, Z. Chen, M. Marquis, K. Averyt, M. Tignor & H. Miller). Cambridge, UK: Cambridge University Press.

FracFocus, 2016, The national hydraulic fracturing chemical registry, http://fracfocus.org/

Fung, I., J. John, J. Lerner, E. Matthews, M. Prather, L. P. Steele, and P .J. Fraser, Three-dimensional model synthesis of the global methane cycle, J. Geophys. Res., 96, 13,033-13,065, 1991.

Garny, H., and W. J. Randel (2013), Dynamic variability of the Asian monsoon anticyclone observed in potential vorticity and correlations with tracer distributions, J. Geophys. Res. Atmos., 118, 13,421–13,433, doi:10.1002/2013JD020908.

Helmig, D., Rossabi, S., Hueber, J., Tans, P., Montzka, S.A., Masarie, K., Thoning,K., Plass-Duelmer, C., Claude, A., Carpenter, L.J., Lewis, A.C., Punjabi, S., Reimann, S., Vollmer, M.K., Steinbrecher, R., Hannigan, J.W., Emmons, L.K., Mahieu, E., Franco, B., Smale, D. and Pozzer, A. : Reversal of global atmospheric ethane and propane trends largely due to US oil and natural gas production", Nature Geoscience, 9, 490-495, doi:10.1038/ngeo2721, 2016

Houweling S., F. J. Dentener, J. Lelieveld, B. Walter, and E. J. Dlugokencky (2000b), The modeling of tropospheric methane: How well can point measurements be reproduced by a global model?, J. Geophys. Res., 105, 8981- 9002

Houweling S., T. Röckmann, I. Aben, F. Keppler, M. Krol, J. F. Meirink, E. J. Dlugokencky, and C. Frankenberg (2006), Atmospheric constraints on global emissions of methane from plants, Geophys. Res. Lett., 33, L15821, doi:10.1029/2006GL026162.

IPCC, 2013: Summary for Policymakers. In: Climate Change 2013: The Physical Science Basis. Contribution of Working Group I to the Fifth Assessment Report of the Intergovernmental Panel on Climate Change [Stocker, T.F., D. Qin, G.-K. Plattner, M. Tignor, S.K. Allen, J. Boschung, A. Nauels, Y. Xia, V. Bex and P.M. Midgley (eds.)], Cambridge University Press, Cambridge, United Kingdom and New York, NY, USA.~~)]~~.

IPCC, 2014: Climate Change 2014: Synthesis Report. Contribution of Working Groups I, II and III to the Fifth Assessment Report of the Intergovernmental Panel on Climate Change [Core Writing Team, R.K. Pachauri and L.A. Meyer (eds.)]. IPCC, Geneva, Switzerland, 151 pp.

~~Cambridge University Press, Cambridge, United Kingdom and New York, NY, USA.~~Jöckel P., A. Kerkweg, A. Pozzer, R. Sander, H. Tost, H. Riede, A. Baumgaertner, S. Gromov, and B. Kern, Development cycle 2 of the Modular Earth Submodel System (MESSy2), Geosci. Model Dev., 3, 717-752, doi:10.5194/gmd-3-717-2010, 2010

Jöckel P., Tost, H., Pozzer, A., Brühl, C., Buchholz, J., Ganzeveld, L., Hoor, P., Kerkweg, A., Lawrence, M. G., Sander, R., Steil, B., Stiller, G., Tanarhte, M., Taraborrelli, D., van Aardenne, J., and Lelieveld, J.: The atmospheric chemistry general circulation model ECHAM5/MESSy1: consistent simulation of ozone from the surface to the mesosphere, Atmos. Chem. Phys., 6, 5067- 5104, doi:10.5194/acp-6-5067-2006, 2006.

Kai F.M, Stanley C. Tyler, J.T. Randerson, and D.R. Blake, Reduced methane growth rate explained by decreased Northern Hemisphere microbial sources, Nature 476, 194–197, 2011, doi:10.1038/nature10259.

Karion A., et al. (2013), Methane emissions estimate from airborne measurements over a western United States natural gas field, Geophys. Res. Lett., 40, 4393-4397, doi:10.1002/grl.50811.

Kerkweg, A., Buchholz, J., Ganzeveld, L., Pozzer, A., Tost, H., and Jöckel, P.: Technical Note: An implementation of the dry removal processes DRY DEPosition and SEDImentation in the Modular Earth Submodel System (MESSy), Atmos. Chem. Phys., 6, 4617-4632, https://doi.org/10.5194/acp-6-4617-2006, 2006.

Krol, M., de Bruine, M., Killaars, L., Ouwersloot, H., Pozzer, A., Yin, Y., Chevallier, F., Bousquet, P., Patra, P., Belikov, D., Maksyutov, S., Dhomse, S., Feng, W., and Chipperfield, M. P.: Age of Air as a diagnostic for transport time-scales in global models, Geosci. Model Dev. Discuss., https://doi.org/10.5194/gmd-2017-262, 2017.

Lelieveld J., P. J. Crutzen, and F. J. Dentener, Changing concentration, lifetime and climate forcing of atmospheric methane, Tellus, 50B, 128-150, 1998.

Lelieveld, J., S. Gromov, A. Pozzer, and D. Taraborrelli, Global tropospheric hydroxyl distribution, budget and reactivity, Atmos. Chem. Phys., 16, 12477-12493, 2016.

Montzka, S., M. Krol, E. Dlugokencky, B. Hall, P. Jöckel, and J. Lelieveld, Small inter-annual variability of global atmospheric hydroxyl, Science, 331, 67-69, 2011.

Nisbet ~~G., Edward J. Dlugokencky, and P. Bousquet, Methane on the Rise–Again, Science 31 Jan 2014 : 493–495~~, E. G., et al. (2016): Rising atmospheric methane: 2007–2014 growth and isotopic shift, Global Biogeochem. Cycles, 30, 1356–1370, doi:10.1002/2016GB005406.

Olivier Jos G.J. , Jan J.M. Berdowski, Jeroen A.H.W. Peters, Joost Bakker, Antoon J.H. Visschedijk and JanPieter J. Bloos, Applications of EDGAR, RIVM report 773301001 / NRP report 410 200 051, 2001/2002

Prinn, R. G., R.F. Weiss, P.B. Krummel, S. O'Doherty, P.J. Fraser, J. Muhle, S. Reimann, M.K. Vollmer, P.G. Simmonds, M. Maione, J. Arduini, C.R. Lunder, N. Schmidbauer, D. Young, H.J. Wang, J. Huang, M. Rigby, C.M. Harth, P.K. Salameh, T.G Spain, L.P. Steele, T. Arnold, J. Kim, O. Hermansen, N. Derek, B. Mitrevski, and R. Langenfelds (2016), The ALE / GAGE AGAGE Network, Carbon Dioxide Information Analysis Center (CDIAC), Oak Ridge National Laboratory (ORNL), U.S. Department of Energy (DOE).

Prinn R. G., R.F. Weiss, P. J. Fraser, P. G. Simmonds, D. M. Cunnold, S. O'Doherty, P. K. Salameh, L. W. Porter, P. B. Krummel, R. H. J. Wang, B. R. Miller, C. Harth, B. R. Greally, F. A. Van Woy, L. P. Steele, J. Mühle, G. A. Sturrock, F. N. Alyea, J. Huang, and D. E. Hartley (2013), The ALE / GAGE AGAGE Network, Carbon Dioxide Information Analysis Center (CDIAC), Oak Ridge National Laboratory (ORNL), U.S. Department of Energy (DOE).

Prinn R. G., R.F. Weiss, P. J. Fraser, P.G. Simmonds, D.M. Cunnold, F.N. Alyea, S. O'Doherty, P. Salameh, B.R. Miller, J. Huang, R.H.J. Wang, D.E. Hartley, C. Harth, L.P. Steele, G. Sturrock, P.M. Midgley, and A. McCulloch, A History of Chemically and Radiatively Important Gases in Air deduced from ALE/GAGE/AGAGE, J. Geophys. Res., 105, 17,751- 17,792, 2000

Prinn R. G., et al~~.~~., "The ALE/GAGE/AGAGE network." carbon (1978).

Randerson, J. T., G.R. van der Werf, L. Giglio, G.J. Collatz, and P.S. Kasibhatla. 2018. Global Fire Emissions Database, Version 4, (GFEDv4). ORNL DAAC, Oak Ridge, Tennessee, USA. https://doi.org/10.3334/ORNLDAAC/1293

Rauthe-Schöch A., Baker A. K., Schuck T.J., Brenninkmeijer C.A.M., Zahn A., Hermann M., Stratmann G., Ziereis H., van Velthoven P.F.J., and Lelieveld J.: Trapping, chemistry and export of trace gases in the South Asian summer monsoon observed during CARIBIC flights in 2008, Atmos. Chem. Phys., 16, 3609-3629, doi:10.5194/acp-16-3609-2016, 2016.

Rigby, M., R. G. Prinn, P. J. Fraser, P. G. Simmonds, R. L. Langenfelds, J. Huang, D. M. Cunnold, L. P. Steele, P. B. Krummel, R. F. Weiss, S. O'Doherty, P. K. Salameh, H. J. Wang, C. M. Harth, J. Mühle, and L. W. Porter, Renewed growth of atmospheric methane, Geophys. Res. Lett., 35(L22805), doi:10.1029/2008GL036037, 2008.

Rigby, M., S. A. Montzka, R. G. Prinn, J. W. C. White, D. Young, S. O'Doherty, M. F. Lunt, A. L. Ganesan, A. J. Manning, P. G. Simmonds, P. K. Salameh, C. M. Harth, J. Mühle, R. F. Weiss, P. J. Fraser, L. P. Steele, P. B. Krummel, A. McCulloch, and S. Park, Role of atmospheric oxidation in recent methane growth, Proceedings of the National Academy of Sciences, 114(21), 5373-5377, doi: 10.1073/pnas.1616426114, 2017.

Roeckner E. et al., Sensitivity of simulated climate to horizontal and vertical resolution in the ECHAM5 atmosphere model, J. Climate, 19, 3771-3791, 2006.

Schaefer, H. et al. A 21st century shift from fossil-fuel to biogenic methane emissions indicated by $^{13}CH_4$. Science 352, 80–84 (2016).

Schuck T. J., K. Ishijima, P. K. Patra, A. K. Baker, T. Machida, H. Matsueda, Y. Sawa, T. Umezawa, C. A. M. Brenninkmeijer, and J. Lelieveld (2012), Distribution of methane in the tropical upper troposphere measured by CARIBIC and CONTRAIL aircraft, J. Geophys. Res., 117, D19304, doi:10.1029/2012JD018199.

Simpson, I.J. et al., Long-term decline of global atmospheric ethane concentrations and implications for methane, Nature 488, 490–494 (2012), doi:10.1038/nature11342

Spahni R. et al., Constraining global methane emissions and uptake by ecosystems, Biogeosciences, 8, 1643-1665, doi:10.5194/bg-8-1643-2011, 2011

~~van der Werf, G. R., Randerson, J. T., Giglio, L., van Leeuwen, T. T., Chen, Y., Rogers, B. M., Mu, M., van Marle, M. J. E., Morton, D. C., Collatz, G~~Turner, A. J., D. J. Jacob, J. Benmergui, S. C. Wofsy, J. D. Maasakkers, A. Butz, O. Hasekamp, and S. C. Biraud (2016), A large increase in U.S. methane emissions over the past decade inferred from satellite data and surface observations, *Geophys. Res. Lett.*, *43*, 2218–2224, doi:10.1002/2016GL067987.

Turner, A. J., C. Frankenberg, P. O.Wennberg, and D. J. Jacob, Ambiguity in the causes for decadal trends in atmospheric methane and hydroxyl, Proceedings of the National Academy of Sciences, 114(21), 5367-5372, doi: 10.1073/pnas.1616020114, 2017.

Worden, J. R., A. A. Bloom, S. Pandey, Z. Jiang, H. M. Worden, T. W. Walker, S.

Walter B. and Heimann M., A process-based climate-sensitive model to derive methane emissions from natural wetlands: Application to five wetland sites, sensitivity to model parameters, and climate, GLOBAL BIOGEOCHEMICAL CYCLES, VOL. 14, NO. 3, PAGES 745-765, SEPTEMBER 2000

~~, J., Yokelson, R. J. and Kasibhatla, 5 P. S.: Global fire emissions estimates during 1997–2015, Earth Syst. Sci. Data Discuss., 1–43, doi:10.5194/essd-2016-62, 2017.~~

White J.W.C., B.H. Vaughn, and S.E. Michel (2015), University of Colorado, Institute of Arctic and Alpine Research (INSTAAR), Stable Isotopic Composition of Atmospheric Methane (13C) from the NOAA ESRL Carbon Cycle Cooperative Global Air Sampling Network, 1998-2014, Version: 2016-04-26, Path: ~~.~~http://aftp.cmdl.noaa.gov/data/trace_gases/ch4c13/flask/.

Worden, J. R., A. A. Bloom, S. Pandey, Z. Jiang, H. M. Worden, T. W. Walker, S. Houweling, and T. Röckmann, Reduced biomass burning emissions reconcile conflicting estimates of the post-2006 atmospheric methane budget, Nature Communications, 8(1), 2227, doi: 10.1038/s41467-017-02246-0, 2017.

Acronyms:

EMAC	ECHAM/MESSy Atmospheric Chemistry (EMAC) model
ECHAM	European Center for medium range weather forecast operational model HAMburg version
GAIM	GLOBAL ANALYSIS,INTEGRATION, AND MODELLING
IGBP	International Geosphere-Biosphere Programme
EDGAR	Emissions Database for Global Atmospheric Research
GFED	Global Fire Emissions Database
AGAGE	Advanced Global Atmospheric Gases Experiment
NOAA	National Oceanic and Atmospheric Administration

~~MHD Mace Head, Ireland (53° N, 10° W)~~
~~THD Trinidad Head, California (41° N, 124° W)~~
~~MLO Mauna Loa, Hawaii, in the United States (19.5°N, 155.6°W, 3397 masl)~~
~~RPB Ragged Point, Barbados (13° N, 59° W)~~
~~SMO Cape Mata Tula, American Samoa (14° S, 171° W)~~
~~CGO Cape Grim, Australia (41° S, 145° E)~~

Code	Station Name	Country	Lat °	Lon °	elevation / m
ALT	Alert	Canada	82.45	-62.51	190
ASC	Ascension Island	UK	-7.97	-14.40	85
AZR	Terceira Ile., Azores	Portugal	38.77	-27.38	19
BRW	Barrow, Alaska	USA	71.32	-156.61	11
CGO	Cape Grim, Tasmania	Australia	-40.68	144.69	94
CRZ	Crozet Island	France	-46.43	51.85	197
EIC	Easter Island	Chile	-27.16	-109.43	47
GMI	Mariana Islands	Guam	13.39	144.66	0
HBA	Halley Station,	Antarctica, UK	-75.61	-26.21	30
MLO	Mauna Loa, Hawaii	USA	19.54	-155.58	3397
RPB	Ragged Point	Barbados	13.17	-59.43	15
SEY	Mahe Island,	Seychelles	-4.68	55.53	2
SHM	Shemya Island, Alaska	USA	52.71	174.13	23
SMO	Tutuila, Am. Samoa	USA	-14.25	-170.56	42
SPO	South Pole	USA	-89.98	-24.80	2810
ZEP	Ny-Alesund, Svalbard	Norway, Sweden	78.91	11.89	474

CARIBIC	Civil Aircraft for the Regular observation of the atmosphere Based on an Instrumented Container
AFR	Africa
EUR	Europe
FAE	Far East
IND	India
NAM	North America
SAN	South America north
SAS	South America south
TRO	Tropical wetland methane emissions scenario 2007-2014
SHA	Shale gas production methane emissions scenario 2007-2014
ITCZ	Inter-Tropical Convergence Zone

Tables

CH_4 sources		emission Tg (CH_4)/y		lifetime [y]	Seasonality
Code	**category**	**a priory** [1)]	**final** [6)]		
swa	swamps	133	140	10.08	yes
ani	animals	98	100	8.18	
lan	landfills	68	65	7.25	
ric	rice paddies	60	64	7.79	yes
gas	gas production	48	42	7.86	
bog	bogs	42	40	8.91	yes
coa	coal mining	42	31	9.20	
	oceans + offshore traffic [2)]	17			
	oil production, processing [2)]	8			
	other anthrop. Sources [2,3)]	6			
	volcanoes [2)]	4			
oil	oil related	35	33	7.37	
bib	biomass burning [4)]	20	25	-	yes
ter	termites	19	20	7.94	
bfc	biofuel combustion[5)]	15	16	7.88	
	sum	**580**	**577**	8.45	yes

Table 1:

[1)] Methane emissions (Houweling et al. 2006) for EMAC model input 1997 – 2006 (no-trend period).

~~[1]~~[2)] merged in one category "oil~~"~~ related" by [1)]

~~[2]~~[3)] all EDGAR emission classes related to the use of fossil fuels such as residential heating, onshore traffic, industry, ~~etc.~~

~~[3)]~~ ~~redistribution~~[4)] *GFEDv4s statistics (Randerson et al., 2018)*

[5)] *EDGAR2.0 database (Olivier, 2001).*

[6)] rescaled with respect to minimal station observation to model simulation RMS.

	Flight region:	Europe	Africa	Far East	India	North America	South Am. north	South Am. South	Globe
	Acronym:	EUR	AFR	FAE	IND	NAM	SAN	SAS	ALL
	No-trend period mean 1997-2006:								
C1	**observations**	1.783E-06	1.781E-06	1.793E-06	1.788E-06	no flights	1.786E-06	1.778E-06	1.786E-06
C2	**model**	1.790E-06	1.783E-06	1.792E-06	1.793E-06		1.785E-06	1.777E-06	1.788E-06
C3	**RMS %**	1.23	0.69	1.24	0.80		0.75	0.76	1.01
C4	**R^2**	0.82	0.43	0.62	0.67		0.60	0.64	0.65
C5	**samples %**	18.1	4.7	21.5	31.5	0.0	10.5	13.6	100.00
	Trend phase mean 2007-2014:								
T1	**observations**	1.791E-06	1.802E-06	1.802E-06	1.811E-06	1.773E-06	1.813E-06	1.839E-06	1.801E-06
T2	**model**	1.796E-06	1.796E-06	1.805E-06	1.806E-06	1.785E-06	1.804E-06	1.818E-06	1.800E-06
T3	**RMS %**	1.40	1.08	1.44	1.04	1.70	1.03	1.44	1.31
T4	**R^2**	0.84	0.58	0.81	0.72	0.84	0.59	0.29	0.80
T5	**samples %**	25.7	6.9	20.4	8.7	10.3	24.6	3.5	100

~~**Table 2:** Statistical evaluation of AGAGE/NOAA ground station methane samples versus EMAC model simulations using optimized emissions.~~

~~Table 3~~

Table 2: Statistical evaluation of CARIBIC flight methane samples versus EMAC model simulations using optimized emissions.